High Power Lasers in Astrobiology and Physics of Rydberg States

Svatopluk Civiš

J.Heyrovský Institute of Physical Chemistry
AV ČR, Praha 8, Czech Republic

Outline

Rydberg States

- High-*l* (orbital momentum) atomic Rydberg states, n-*l* levels
- Quantum defects for high-*l* states
- The development of the new experimental techniques based on application of high resolution time-resolved Fourier-transform infrared spectroscopy
- Time resolved laboratory spectra of radicals, ions (discharge experiments)
- Fourier transform infrared spectroscopy together with Laser ablation technique - infrared spectra of atoms

PALS

- Application in Astronomy and Astrochemistry
- Atomic spectroscopy-review
- Formation of basic molecules of the RNA world during Heavy bombardment period
- High power laser experiments (PALS)
- Chemistry of stable and unstable products

High-l atomic Rydberg states studied by high resolution time-resolved Fourier-transform infrared spectroscopy

Atomic *nl* levels: an example (Na)

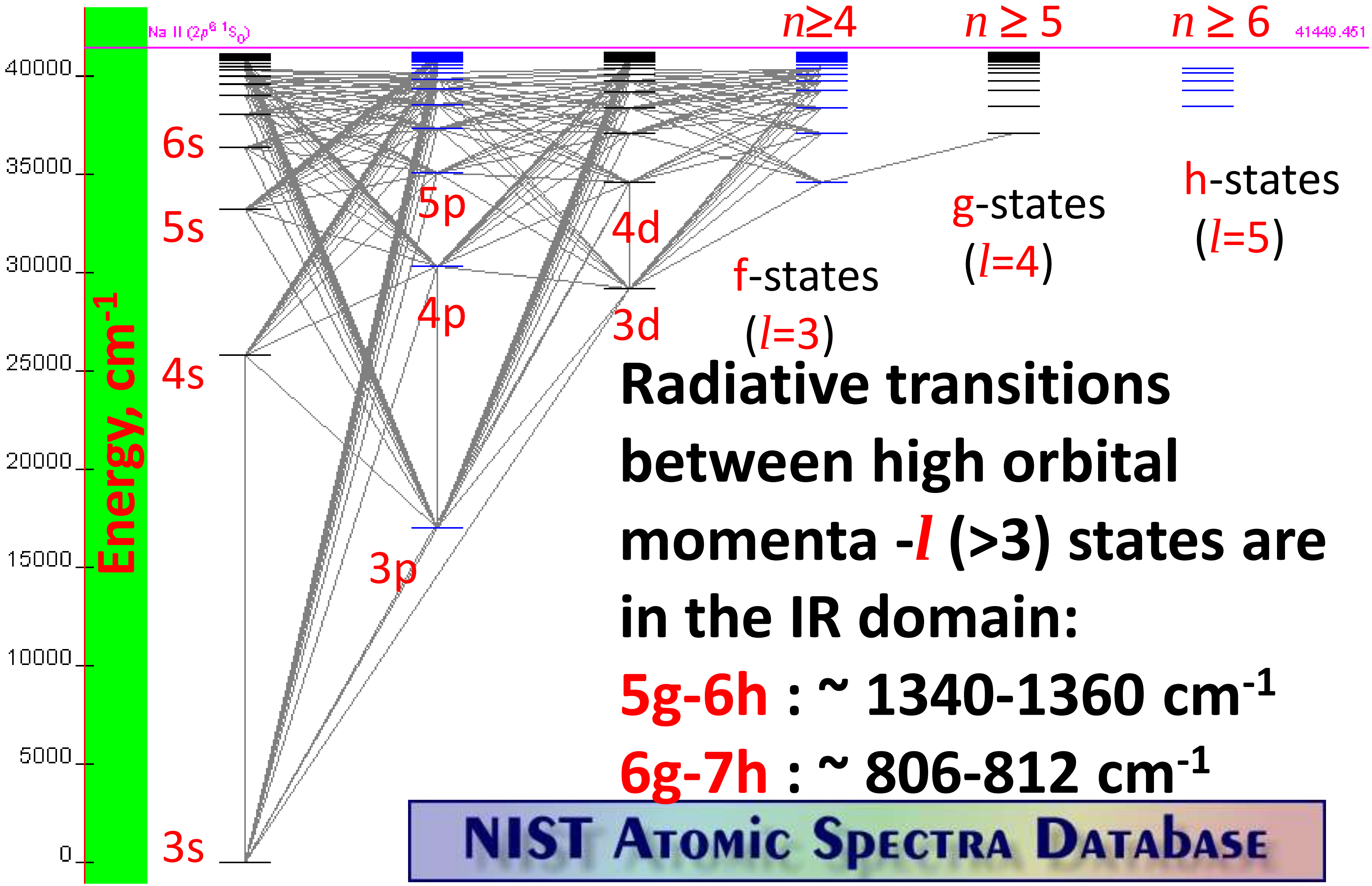

Radiative transitions between high orbital momenta -*l* (>3) states are in the IR domain:

5g-6h : ~ 1340-1360 cm^{-1}

6g-7h : ~ 806-812 cm^{-1}

NIST Atomic Spectra Database

Why the high-*l* states are interesting?

- **Measuring the properties of atoms that control their long-range interactions, such as quadrupole moments and dipole polarizabilities**
- **Challenge to experiment: for He- and Li-like ions, theoretical predictions of high-*l* fine structure appear to be more precise than existing measurements**
- **Challenge to theory: to extend these studies to heavier atoms and ions, where the theoretical calculation of measurable core properties becomes increasingly difficult because of many-body and relativistic effects**
- **IR astronomy: studies of dust-obscured objects and interstellar clouds, cool objects such as dwarfs, disks, or planets and the extended atmospheres of evolved stars, including objects at cosmological distances from the Earth**

Quantum defects for high-*l* states

The discrete spectrum is given by Rydberg formula with the quantum defect μ which is to be determined from the experimental spectra

$$\boxed{E_{nl} = V_{\text{ion}} - \frac{R}{\nu_{nl}^2} = V_{\text{ion}} - \frac{R}{(n-\mu_l)^2}}$$

R is Rydberg constant, V_{ion} is the ionisation threshold

A simple model – polarisation potential $U_c(r) = \alpha_c/r^4$,

where α_c is the atomic core polarisability

$$\mu_{nl} = \frac{2\alpha_c[3 - l(l+1)/n^2]}{l(l+1)(2l-1)(2l+1)(2l+3)}$$

Rapidly decreases with *l*

Fine structure of high-*l* states

The simplest fine-structure correction – spin-orbital splitting

$$\Delta E_{nl} = \frac{R\alpha^2 Z_{\text{eff}}^4}{\nu_{nl}^3 l(l+1)}$$

Rapidly decreases with *n, l*

α ~1/137 is the fine structure constant, Z_{eff} is an effective core charge

n	Fine splitting for different *l* states of Cs atom, cm^{-1}				
	p	d	f	g	h
4	-	-	0.18	-	-
5	-	98	0.15	0.0028	-
6	554	43	0.11	0.016	?
7	181	21	0.74	0.001	?
8	83	12	0.053	0.0009	?
9	45	7.1	0.039	0.013	?
10	27	4.7	0.029	0.0009	?

Time resolved FTIR measurement in the discharge plasma

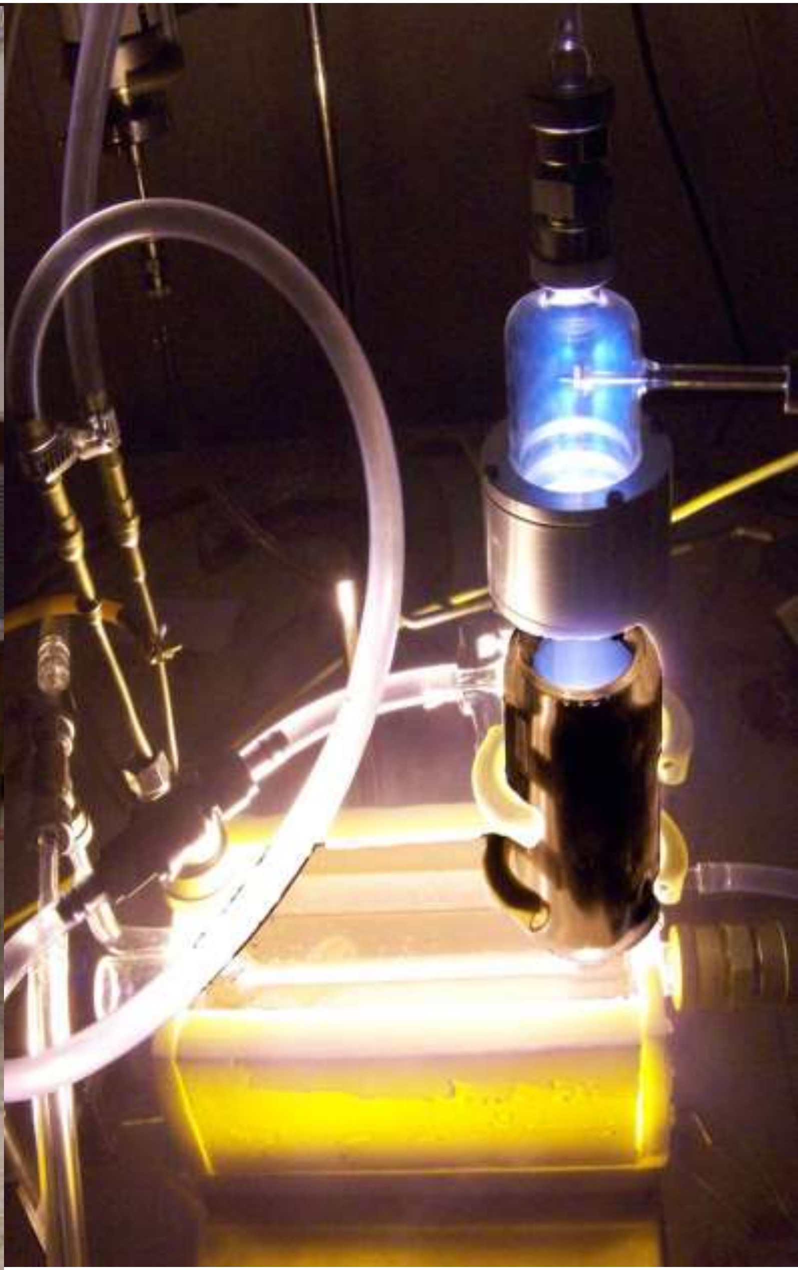

Data collection ?

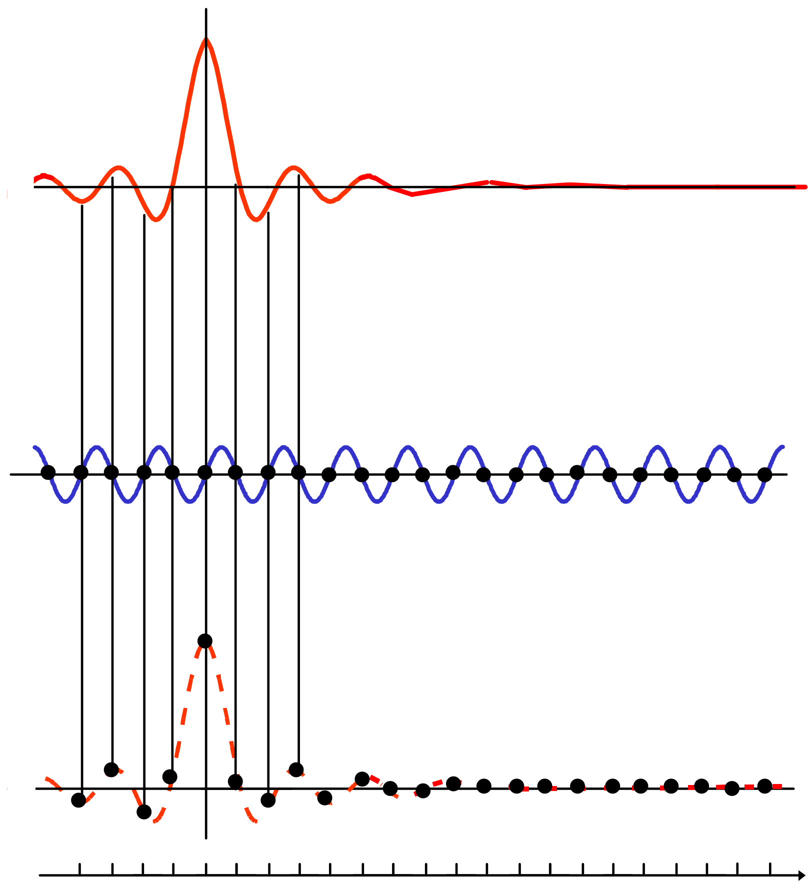

interferograme

Laser interference

Data points from the detector saved by PC

Optical path difference

(given by position of moving mirror)

Fourier transformation

Interferogram

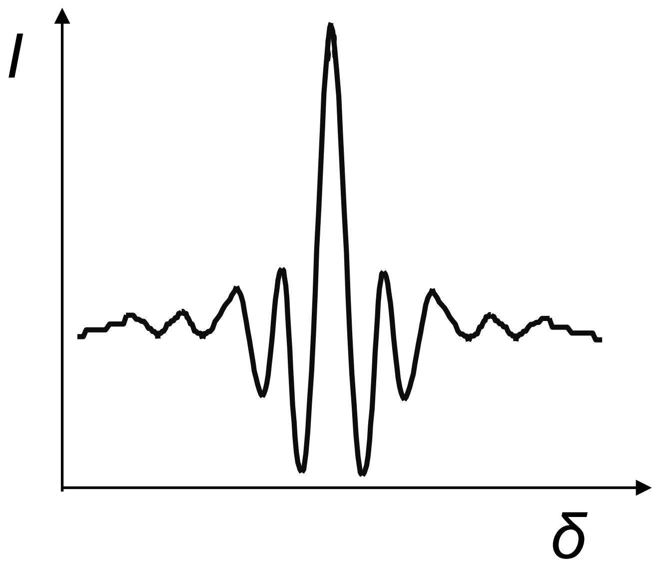

Spectrum

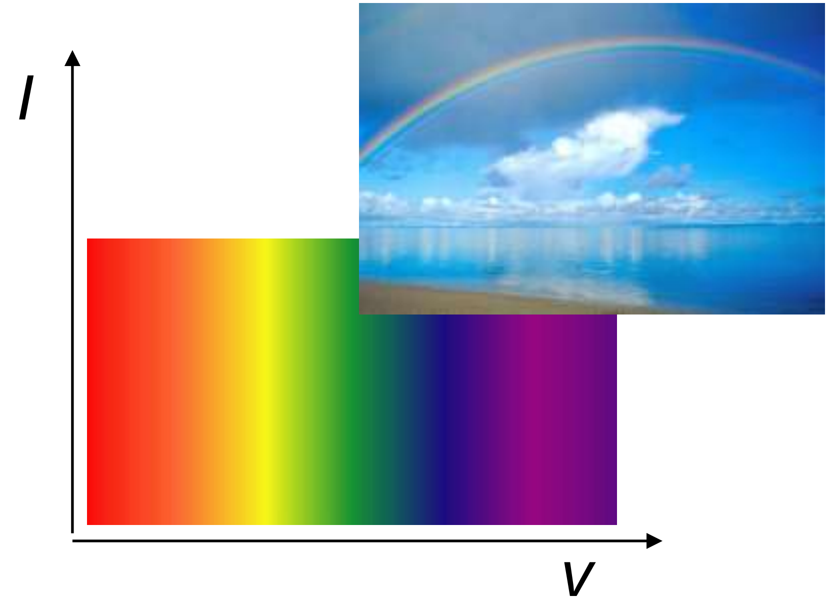

$$I(\delta) = \int_{-\infty}^{\infty} B(\nu)\cos(2\pi\nu\delta)\,d\nu$$

FT

$$B(\nu) = \int_{-\infty}^{\infty} I(\delta)\cos(2\pi\nu\delta)\,d\delta$$

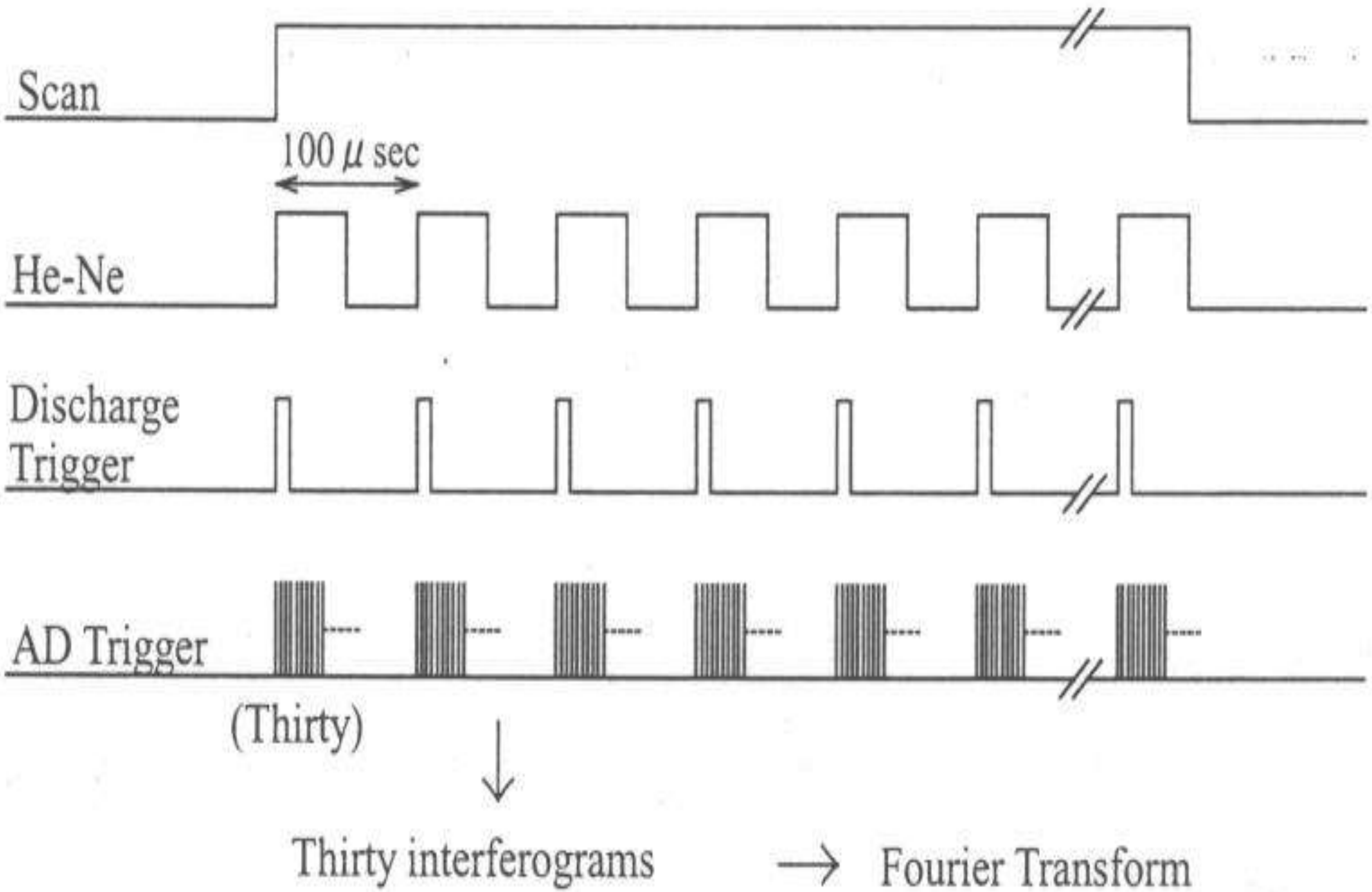
Scan
100 μ sec
He-Ne
Discharge Trigger
AD Trigger
(Thirty)
Thirty interferograms
→ Fourier Transform

He + H_2 discharge plasma

He + H

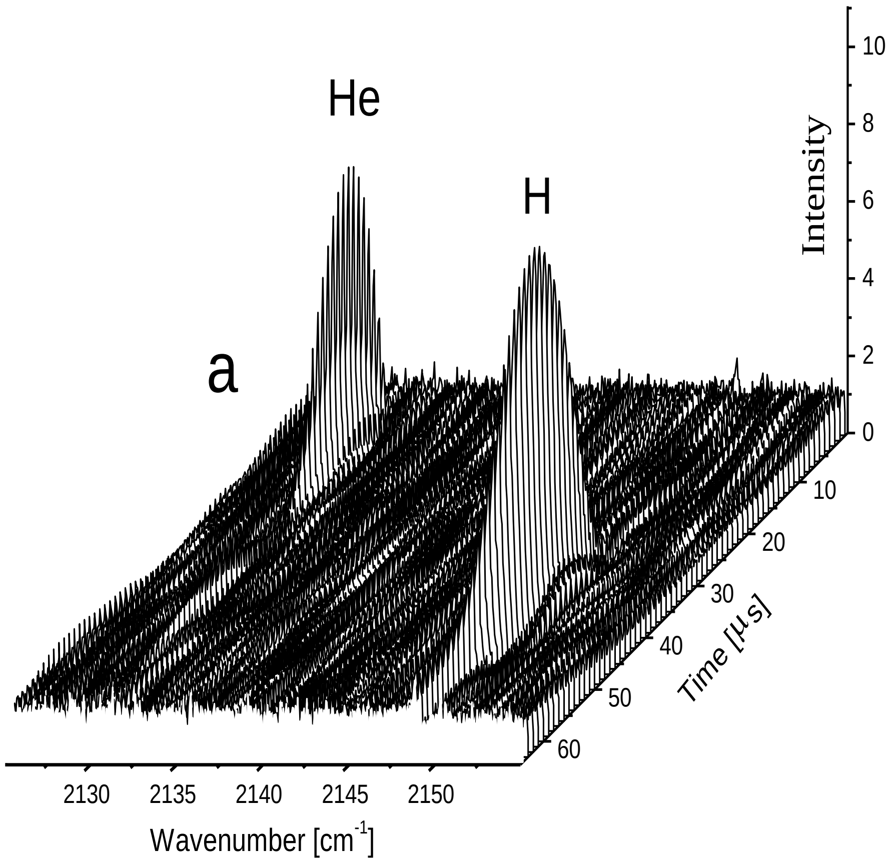

H_3^+

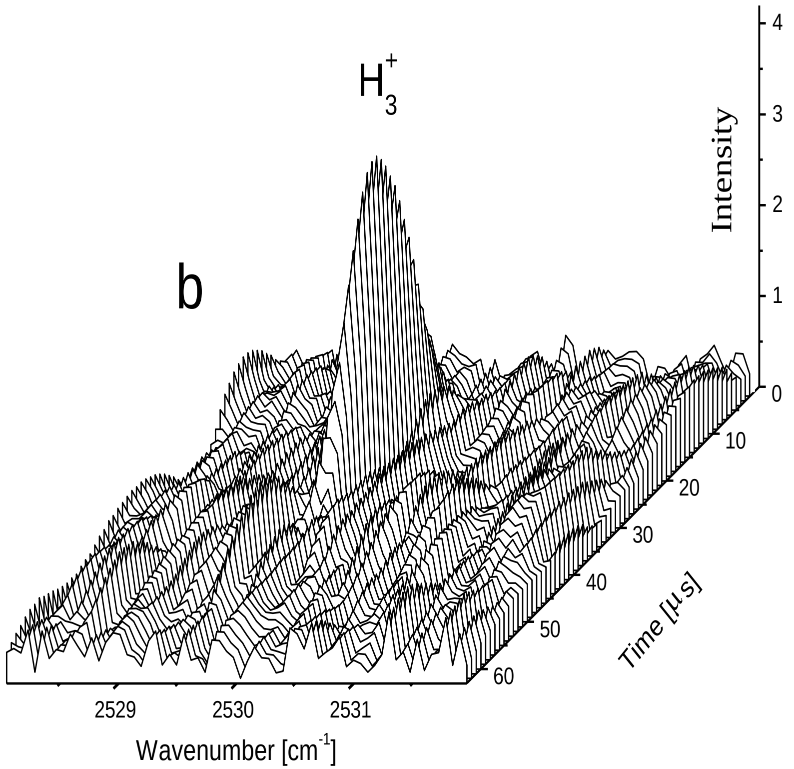

Chemistry of H_3^+ formation using time resolved spectra acquisition

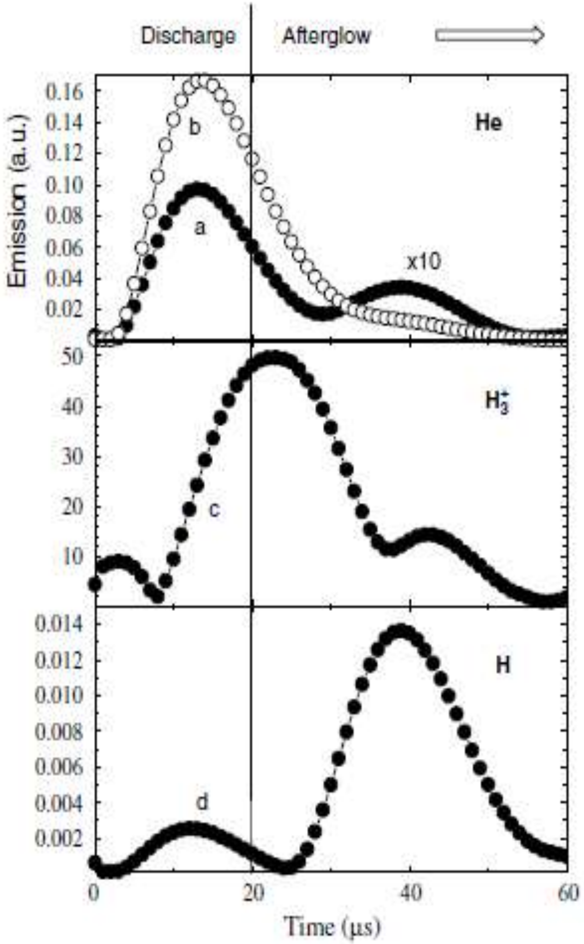

$$He \longrightarrow \ldots \longrightarrow He^*$$ He discharge excitation

$$He^* + H_2 \longrightarrow H_2^+ + e^-$$ Penning ionisation

$$H_2^+ + H_2 \longrightarrow H_3^+ + H$$ H_3^+ formation

Recombination with electron

$$H_3^+ + e^- \longrightarrow H_2(X^1\Sigma_g^+, vJ) + H(1s), \quad \Delta E = 9.2\,eV$$

$$\longrightarrow H(1s) + H(1s) + H(1s). \quad \Delta E = 4.8\,eV$$

S. Civis, P. Kubat, S. Nishida, K. Kawaguchi, ***Chemical Physics Letters***, 418 (2006) 448–453

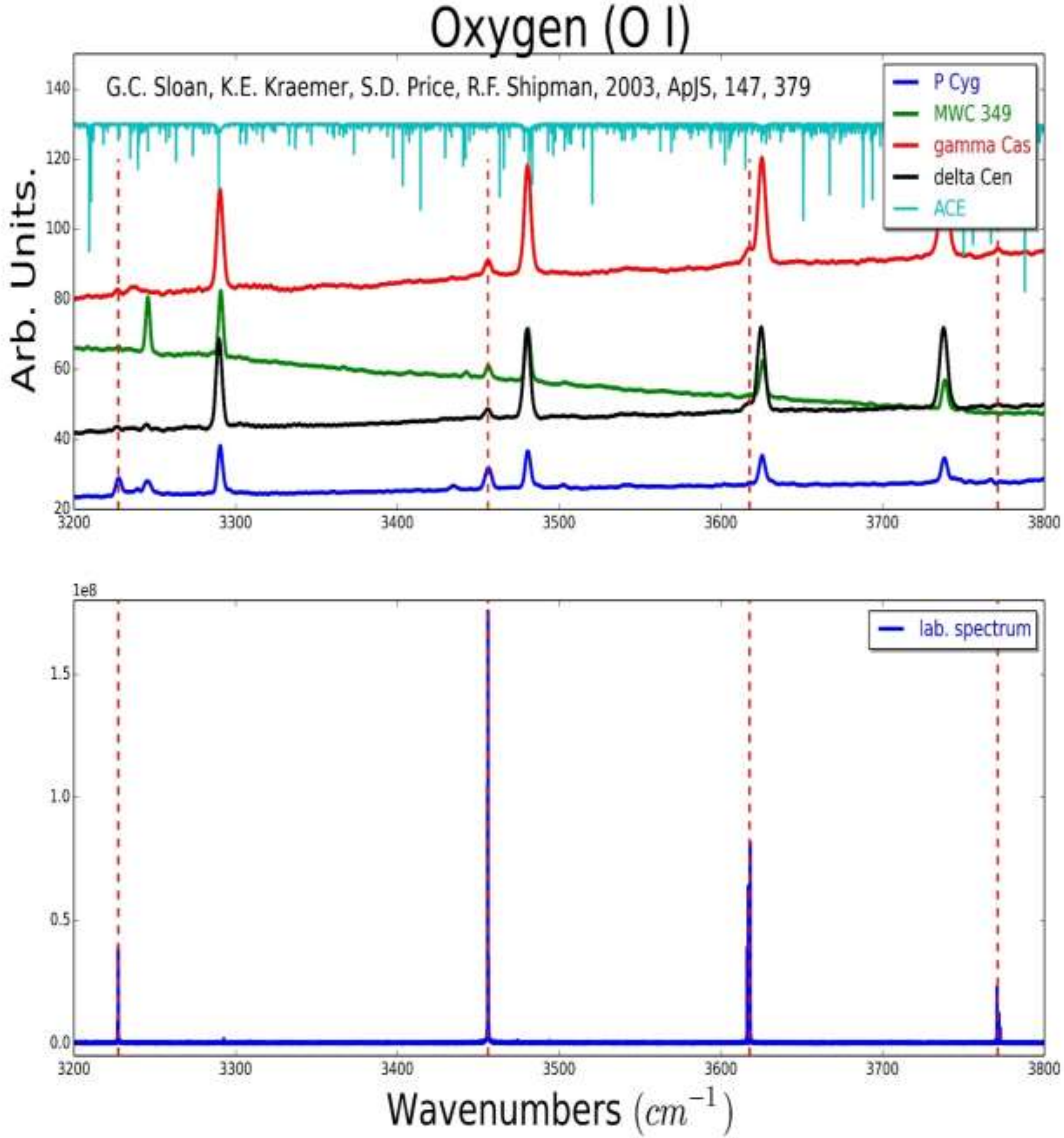
Oxygen (O I)
G.C. Sloan, K.E. Kraemer, S.D. Price, R.F. Shipman, 2003, ApJS, 147, 379
P Cyg
MWC 349
gamma Cas
delta Cen
ACE
Arb. Units.
lab. spectrum
1e8
Wavenumbers (cm^{-1})

Time resolved FTIR measurement in the laser spark (laser ablation)

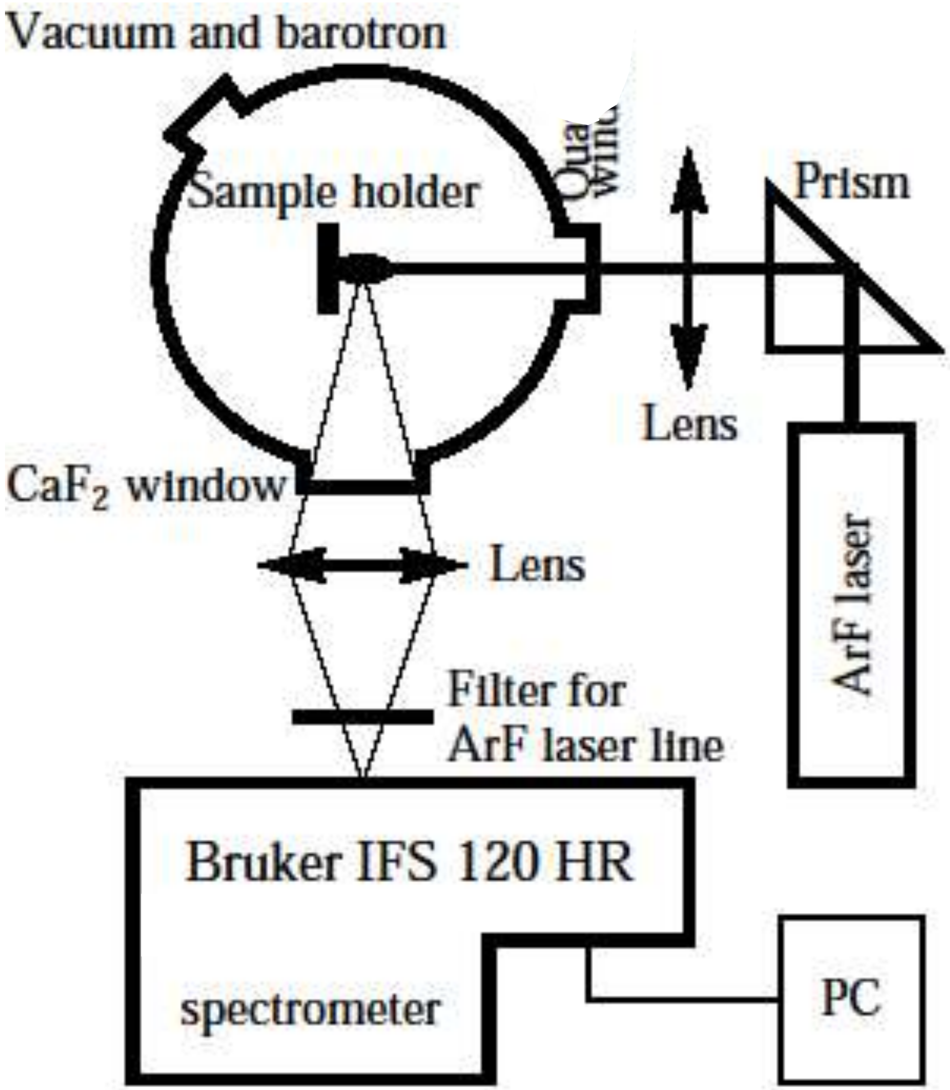

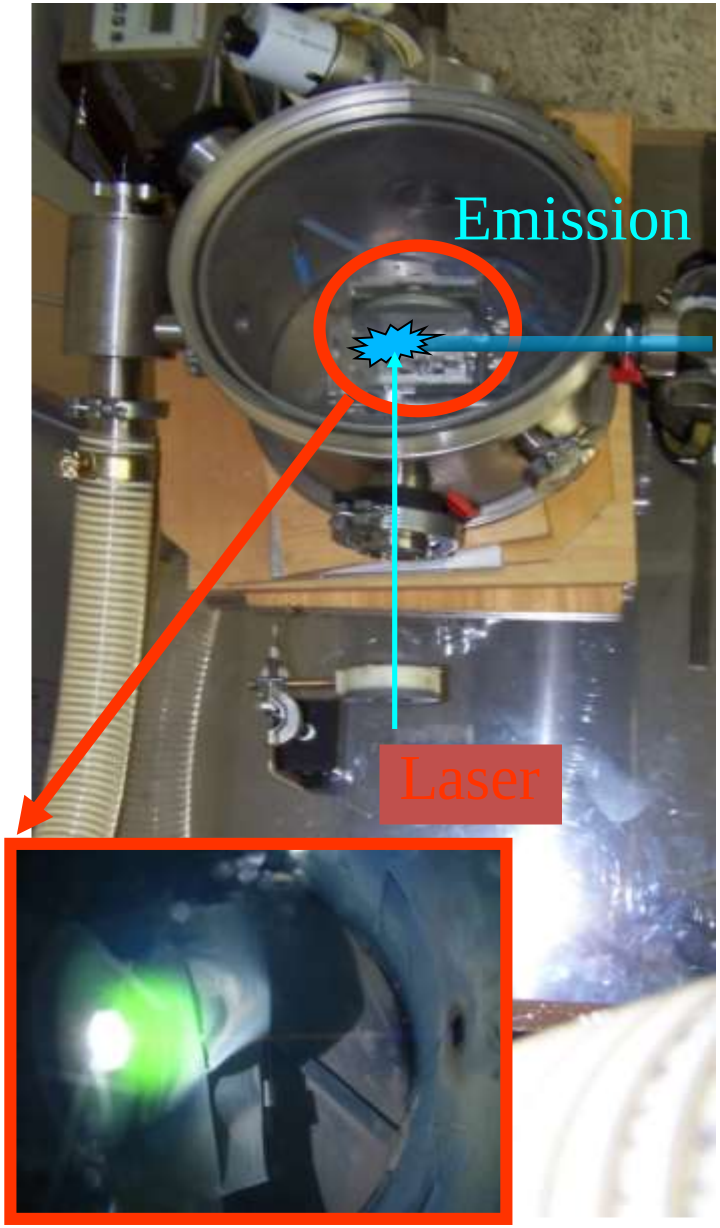

Timing diagram for the interleaved sampling. During the scan, the laser pulse and the AD trigger sampling are induced with a rate of 1/n times of the HeNe laser fringe frequency. The complete interferograms are obtained after n scans.

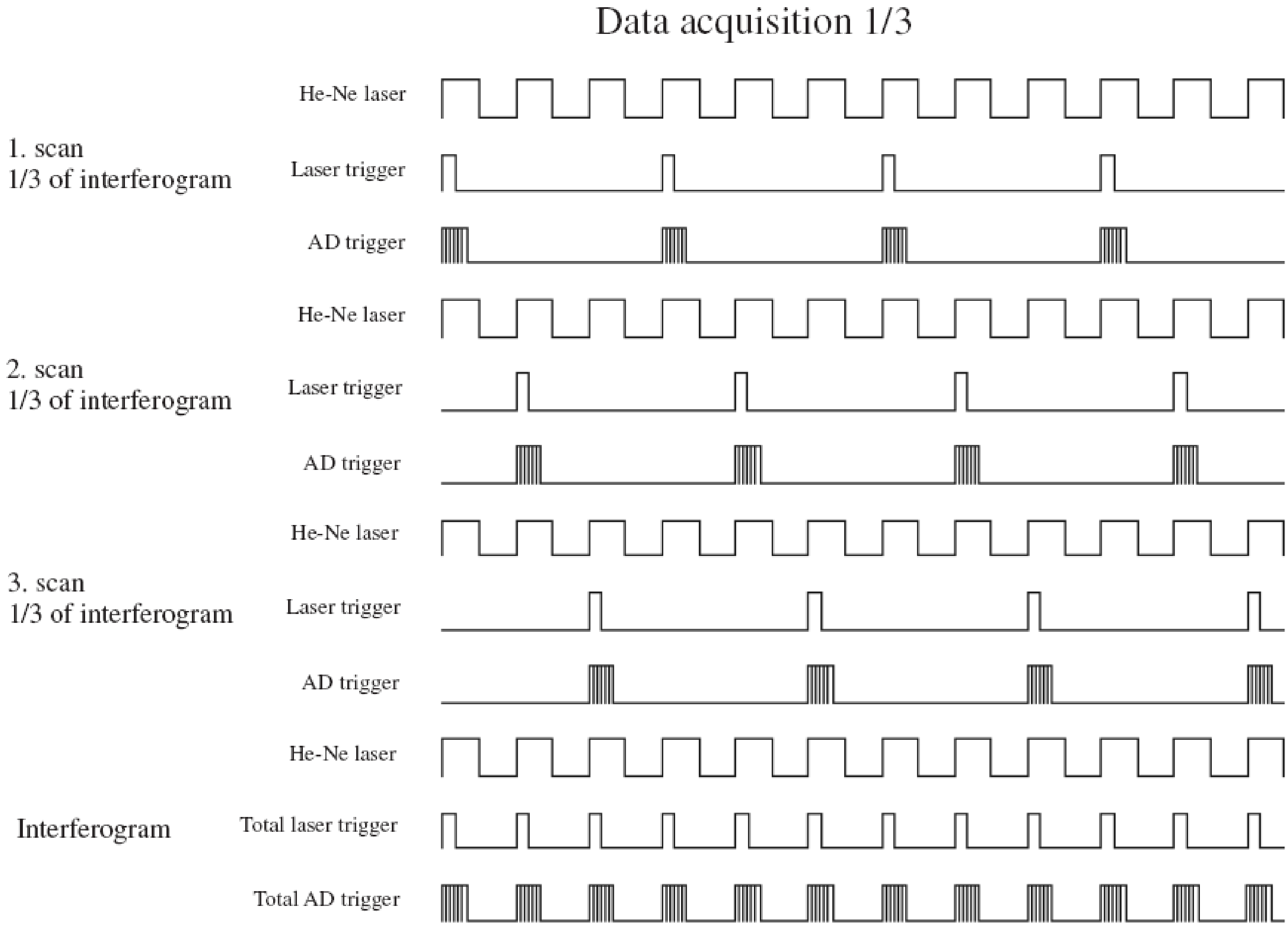

Example of spectra: Cs

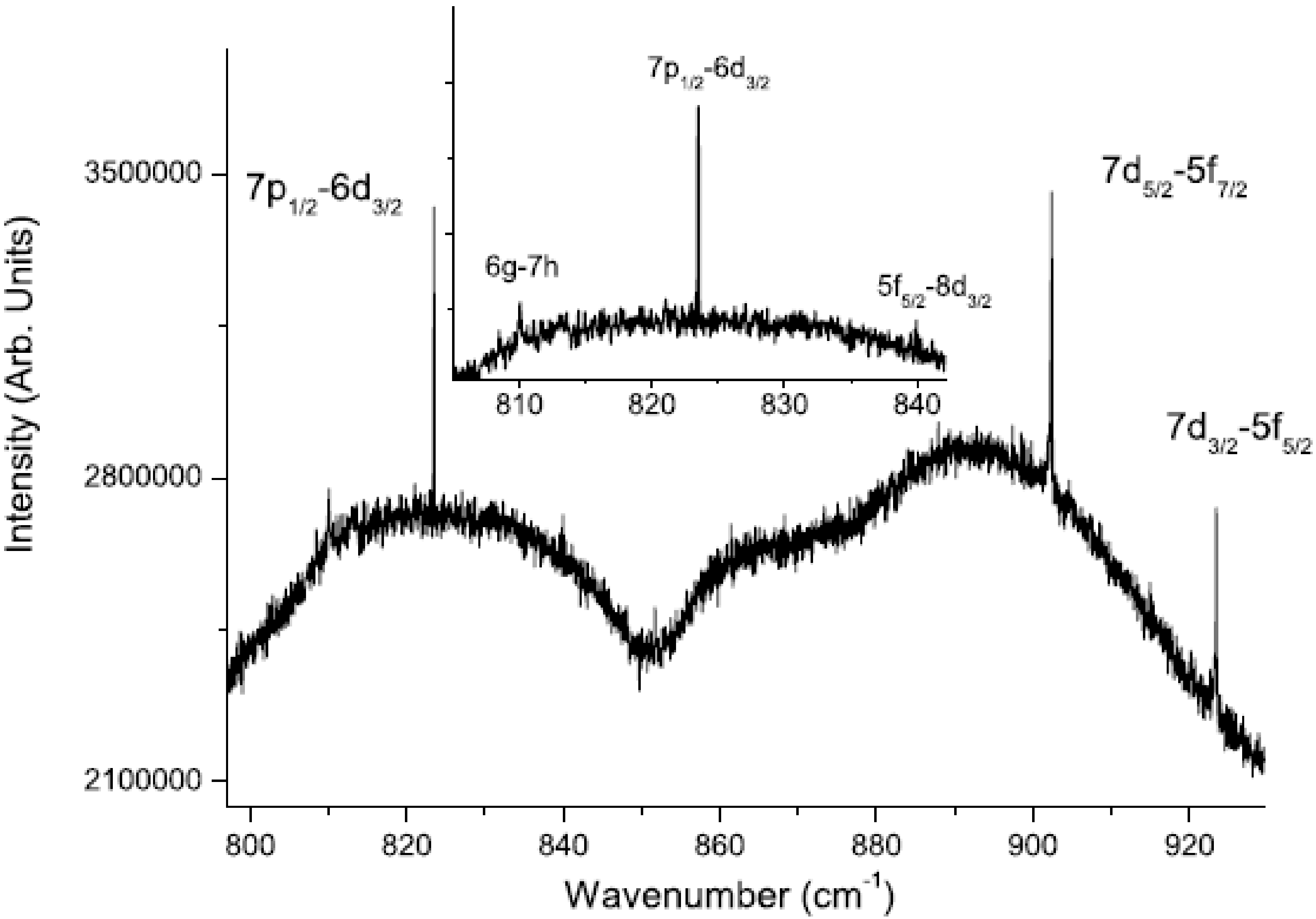

IR astronomy: drawbacks

- **Much lower number of atomic and ionic lines available (relative to the visible and ultraviolet ranges)**
- **Modern laboratory spectral features are lacking for most elements with wavelengths longer than 1 micron**
- **Atlases of stellar spectra often provide only a short list of identified lines. Even in the solar IR atlases there are a number of lines with doubtful or missing identifications.**
- **The reliability of astrophysical calculations cannot be improved without the inclusion of additional atomic lines and higher energy levels**
- **The above IR astronomy facilities cannot be fully utilized without detailed spectroscopic information on atomic line features (line identification, excited (including the high-*l*) level energies, wavelengths and oscillator strengths) in the IR region**
- **Reporting high-resolution laboratory data for atomic spectral features (new IR atomic line wavelengths and identifications, highly-excited levels, and oscillator strengths) is important!**

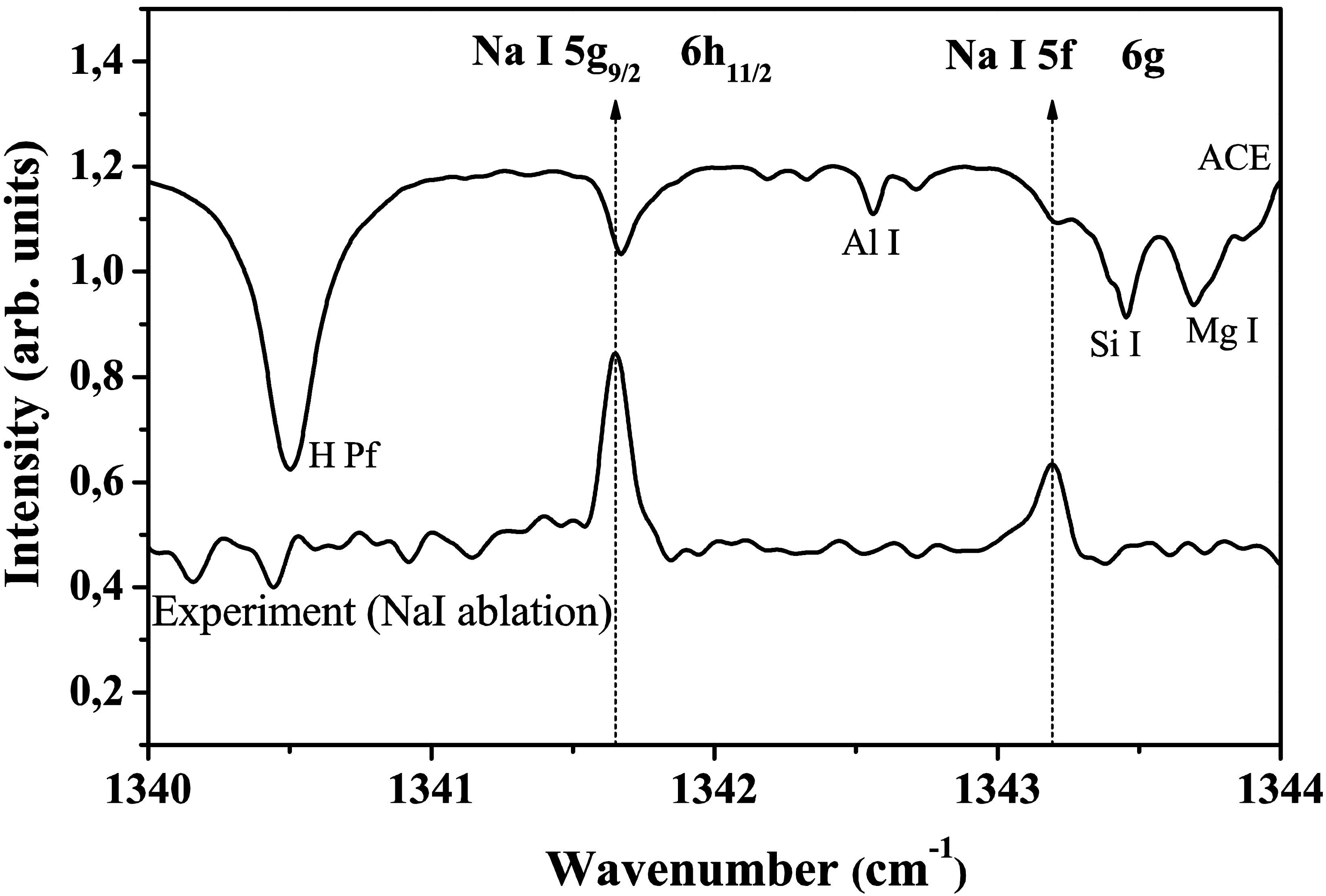

Civiš S., Chernov V.E. *et al*., Astronomy and Astrophysics 2012

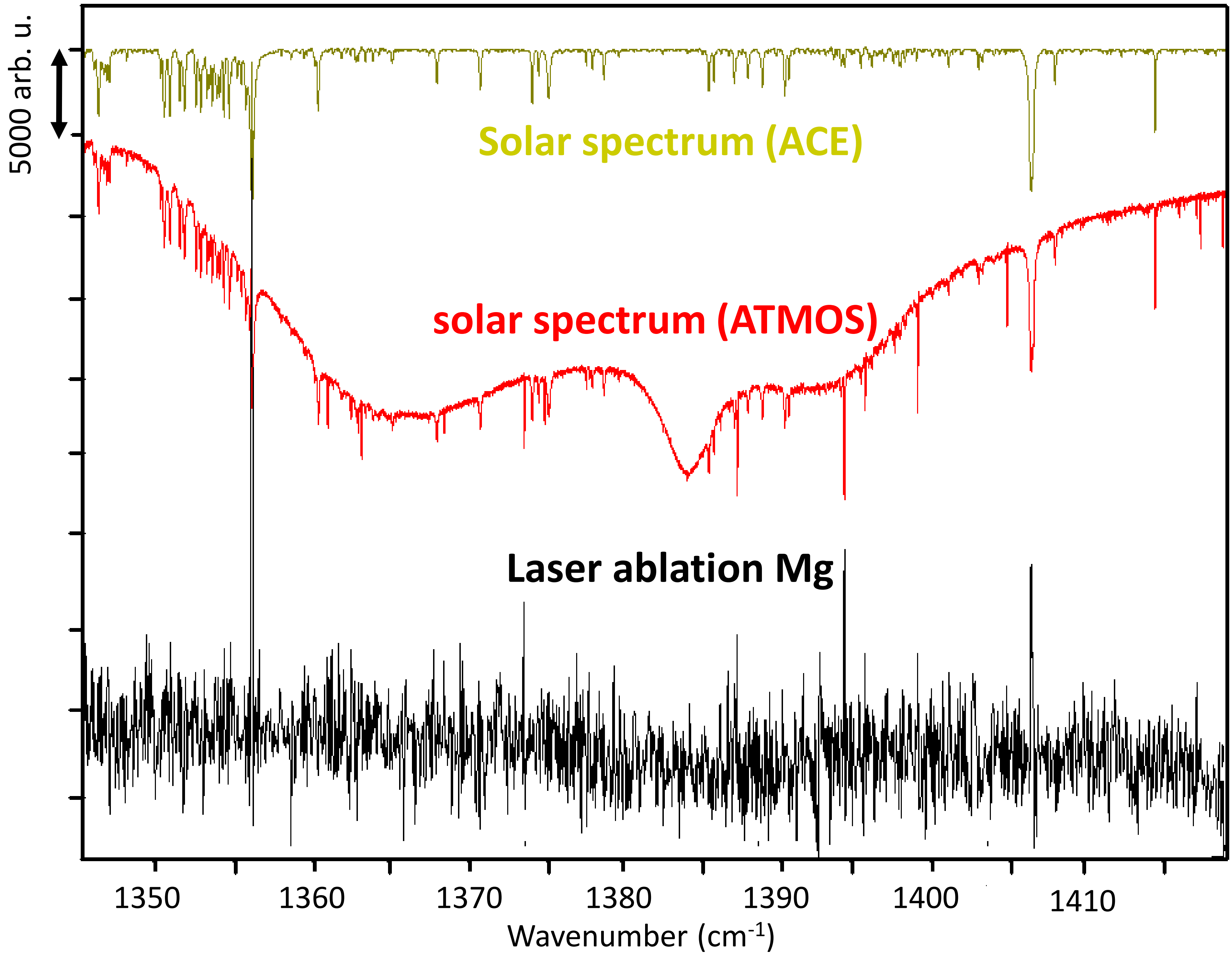
5000 arb. u.
Solar spectrum (ACE)
solar spectrum (ATMOS)
Laser ablation Mg
1350
1360
1370
1380
1390
1400
1410
Wavenumber (cm-1)

Infračervené spektrum hořčíku

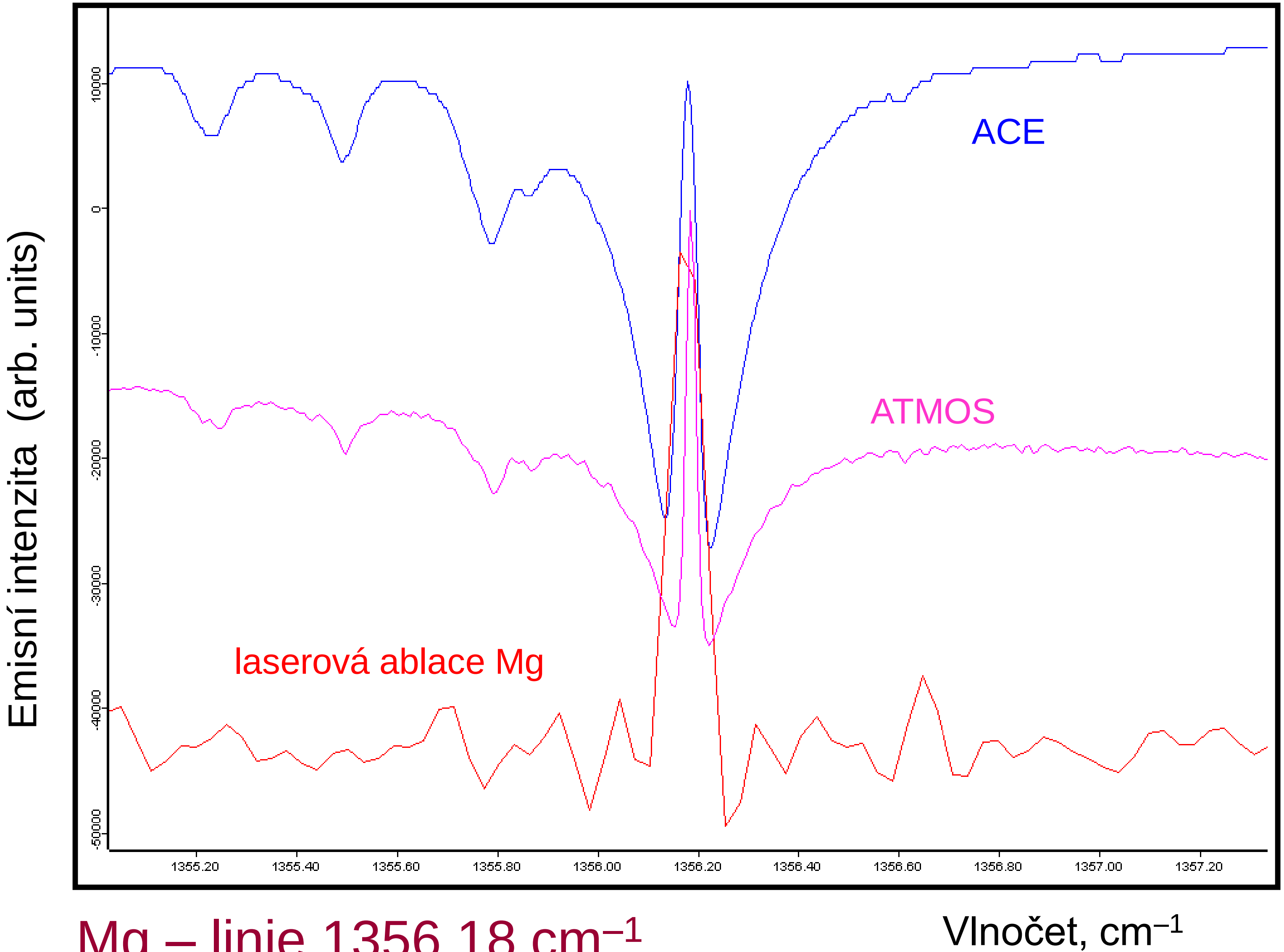

Mg – linie 1356,18 cm^{-1}

Infračervené spektrum křemíku

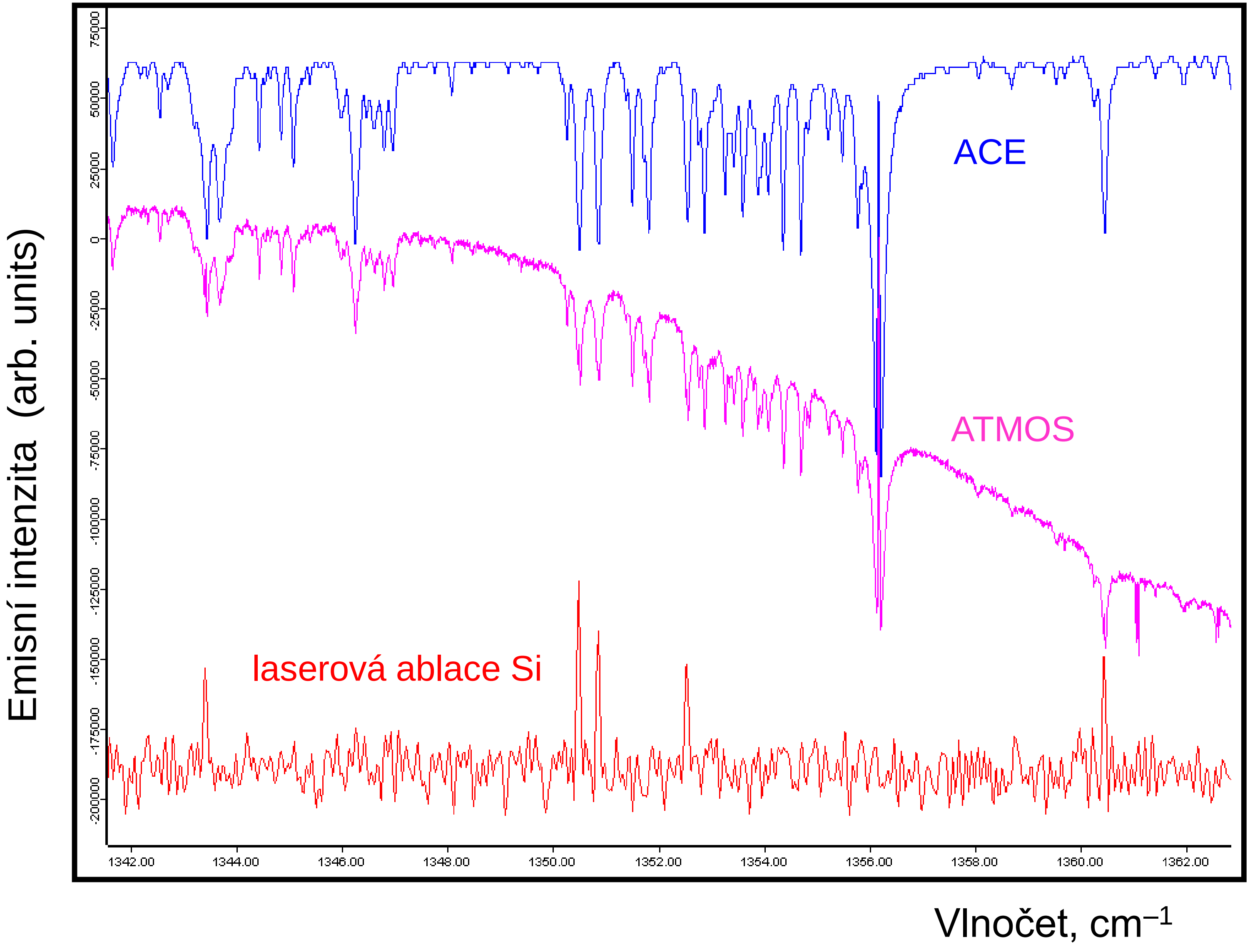

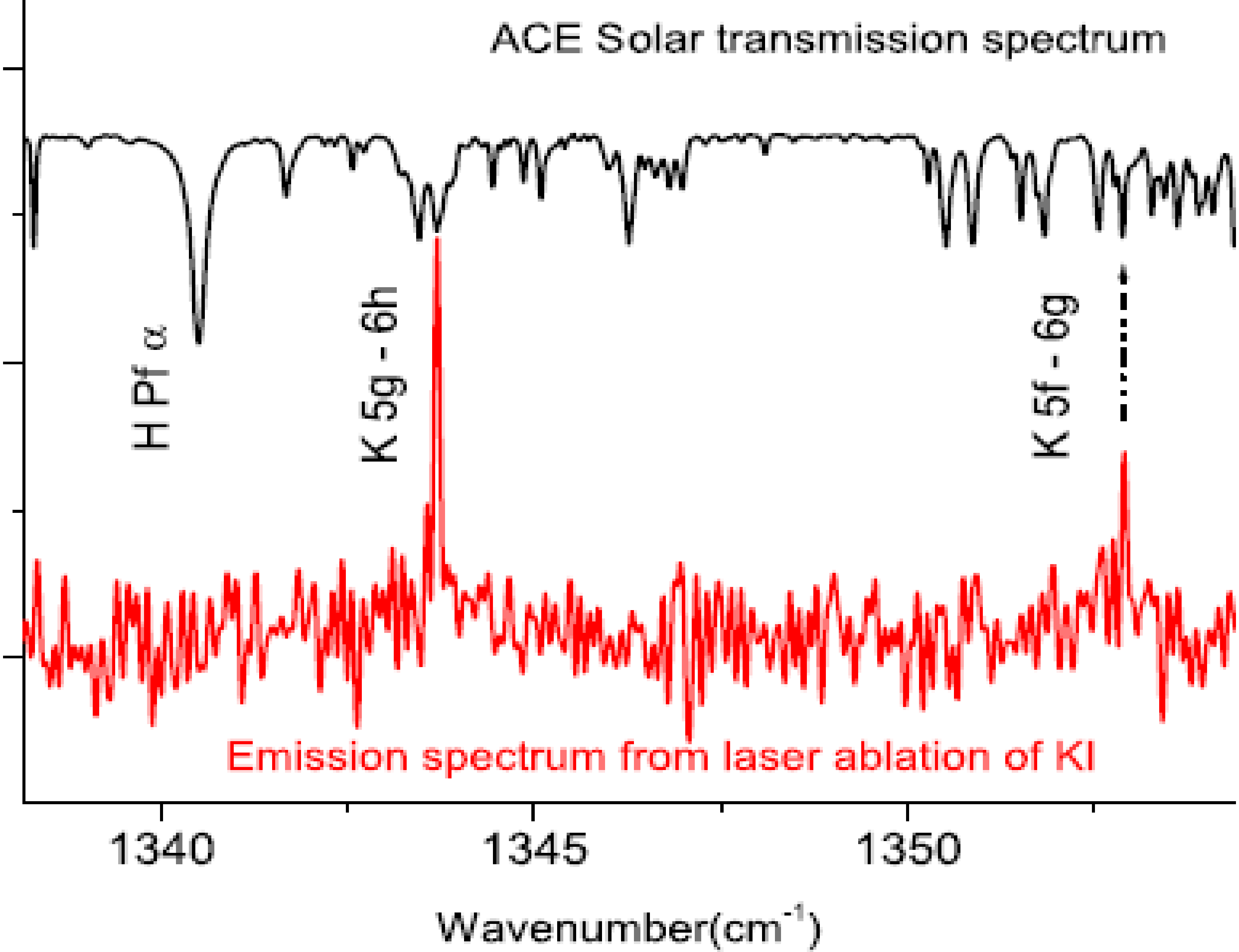

Civiš S., Chernov V.E. *et al*., Astronomy and Astrophysics 2012

Comparison of Arcturus spectrum with FTIR emission spectrum

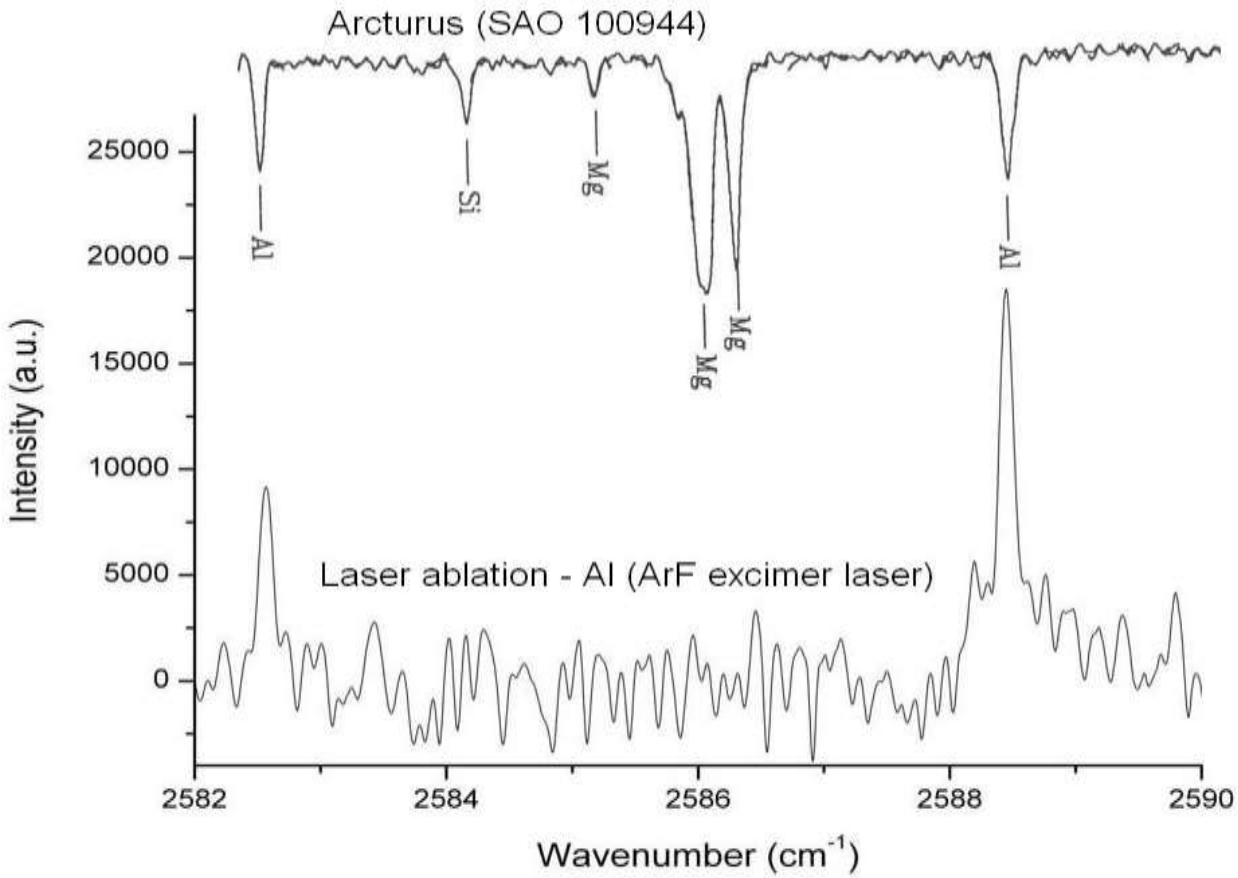

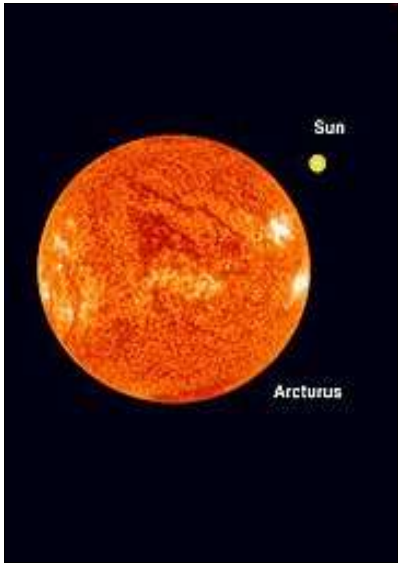

Arcturus' size relative to the Sun

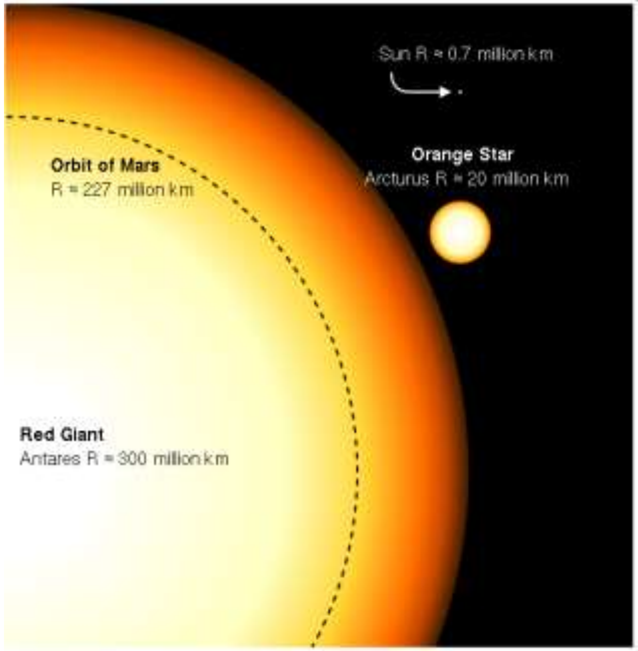

Conclusions

Atom	Lines (total)	New lines	New levels	References
Au	43	32	8	Phys. Rev. A **81**, 012510 (2010)
Ag	18	12	3	Phys. Rev. A **82**, 022502 (2010)
Cu	25	20	4	J. Phys. B **44**, 105002 (2011)
Li	4	4		Astron. & Astrophys. **545**, A61 (2012)
Na	25	17	3	Astron. & Astrophys. **542**, A35 (2012)
K	38	25	3	Astron. & Astrophys. **541**, A125 (2012)
Rb	33	21	6	J. Phys. B **44**, 175002 (2012)
Cs	40	21	2	J.Opt. Soc. Am. B**29**, 112 (2012)
Mg	36	3	2	Astron. & Astrophys. **554**, A24 (2013)
Ca	31	26	12	
Sr	23	19	10	J. Quant. Spectrosc. Radiat. Transf. **129**, 324 (2013)
Zn	54	47	15	J. Quant. Spectrosc. Radiat. Transf. **134**, 64 (2014)
In	34	18	5	J. Anal. At. Spectrom. **29**, 2275 (2014)
Ne	287	26	14	Astron. & Astrophys. **582**, A12 (2015)

James Webb Space Telescope

- 6.6m Telescope
- Successor to Hubble & Spitzer.
- Demonstrator of deployed optics.
- 4 instruments: 0.6 to 28.5 μm
- Passively cooled to < 50 K.
- Named for 2nd NASA Administrator

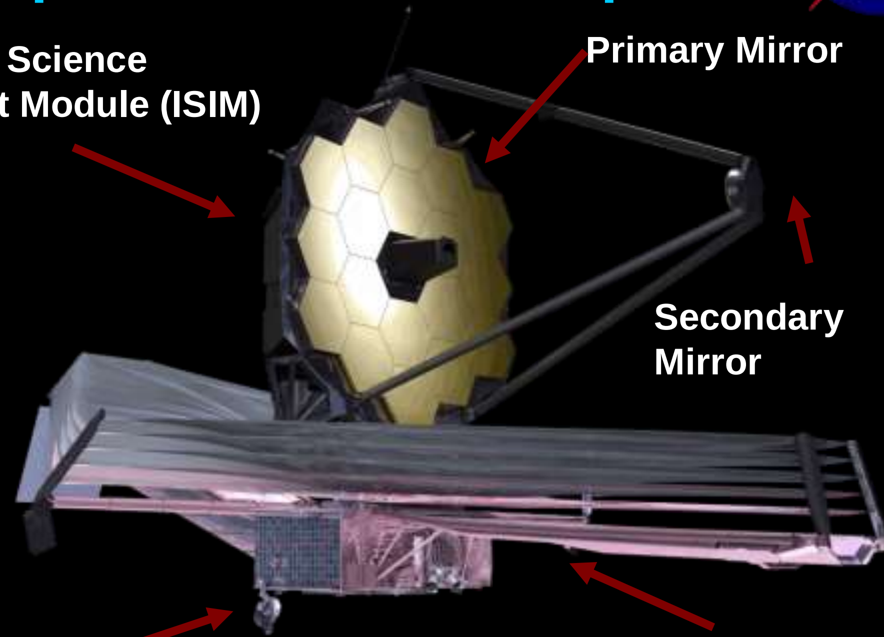

- Complementary to WFIRST, ELT, ALMA, etc
- NASA + ESA + CSA: 14 countries
- Lead: Goddard Space Flight Center
- Prime: Northrop Grumman
- Operations: STScI
- Senior Project Scientist:
  Nobel Laureate John Mather

SCIENCE

Webb Telescope Science Themes

The James Webb Space Telescope will be a giant leap forward in our quest to understand the Universe and our origin cosmic history: from the first luminous glows after the Big Bang to the formation of galaxies, stars, and planets to the evolution of our own solar system.

- First Light & Reionization

JWST will be a powerful time machine with infrared vision that will peer back over 13.5 billion years to see the first stars and galaxies forming out of the darkness of the early universe.

- Assembly of Galaxies

JWST's unprecedented infrared sensitivity will help astronomers to compare the faintest, earliest galaxies to today's grand spirals and ellipticals, helping us to understand how galaxies assemble over billions of years.

- Birth of Stars & Protoplanetary Systems

JWST will be able to see right through and into massive clouds of dust that are opaque to visible-light observatories like Hubble, where stars and planetary systems are being born.

- Planets & Origins of Life

JWST will tell us more about the atmospheres of extrasolar planets, and perhaps even find the building blocks of life elsewhere in the universe. In addition to other planetary systems, JWST will also study objects within our own Solar System.

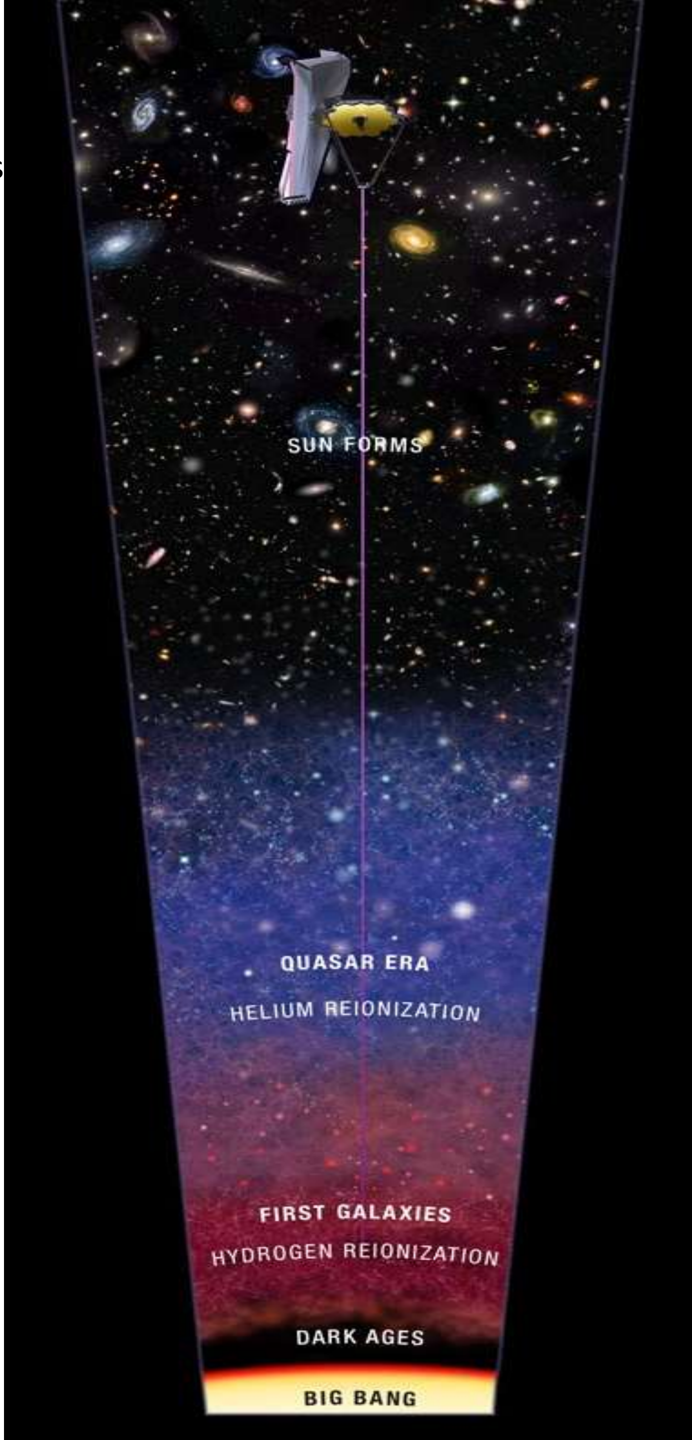

End of the dark ages: first light and reionization

The Assembly of Galaxies

The Birth of Stars and Protoplanetary Systems

Planetary Systems and the Origins of Life

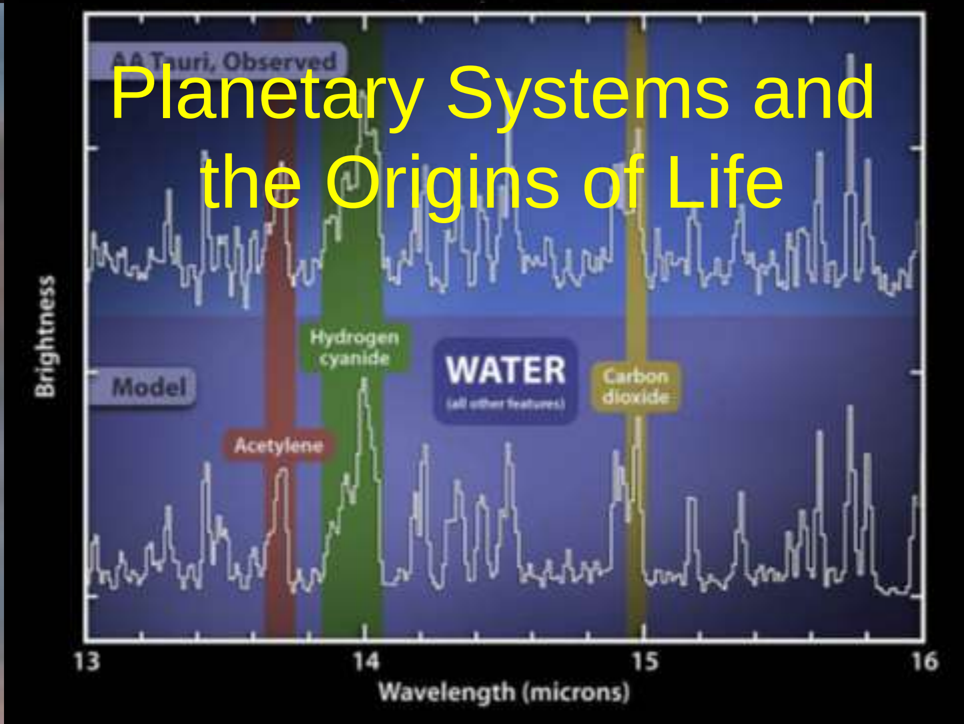

Formation of Basic Molecules of the RNA World during Heavy Bombardment Period

RNA World – the Bases

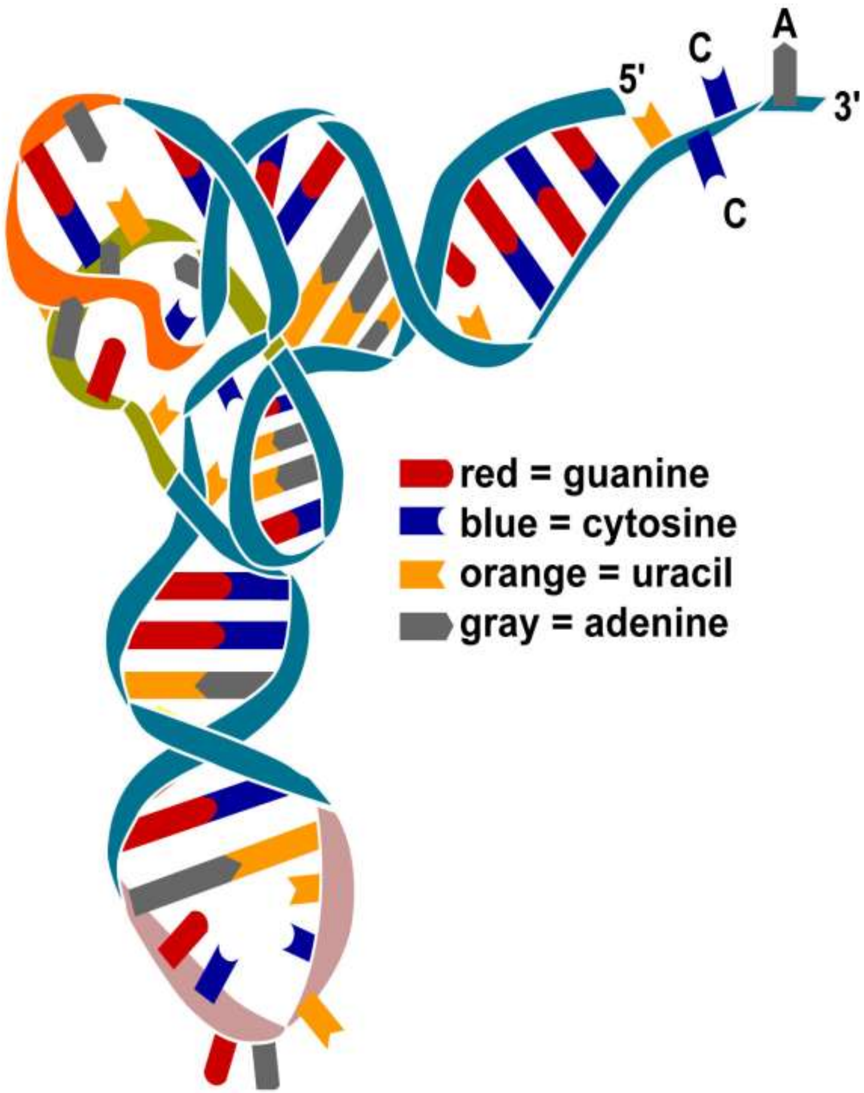

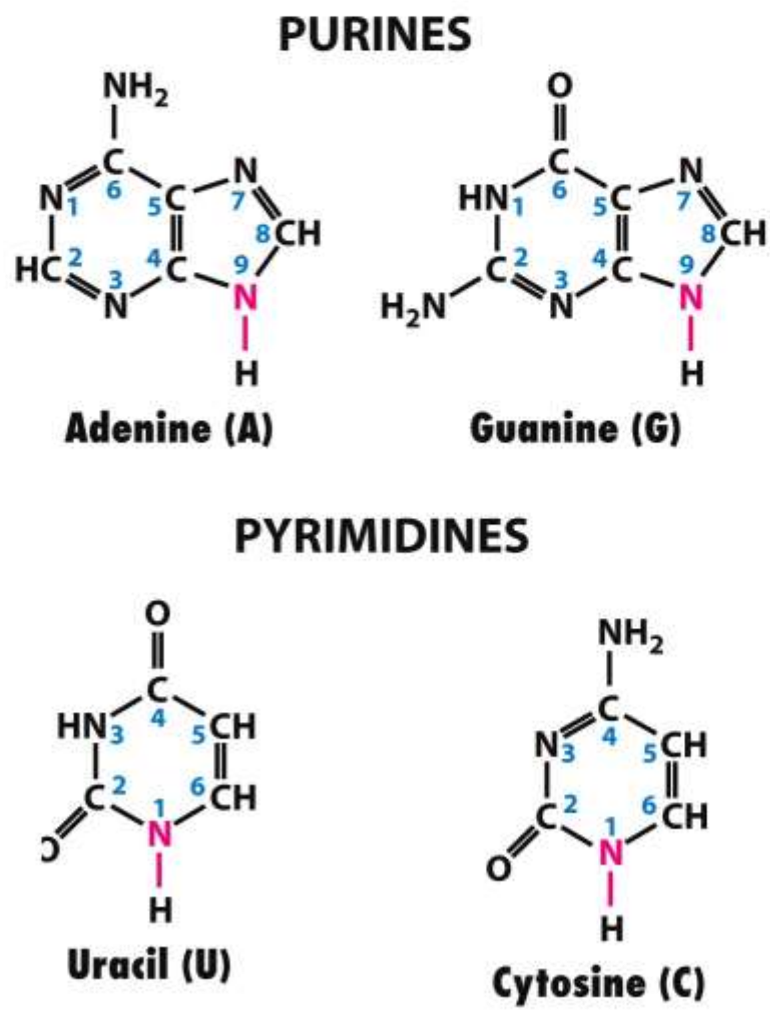

Early and Late Heavy Bombardment

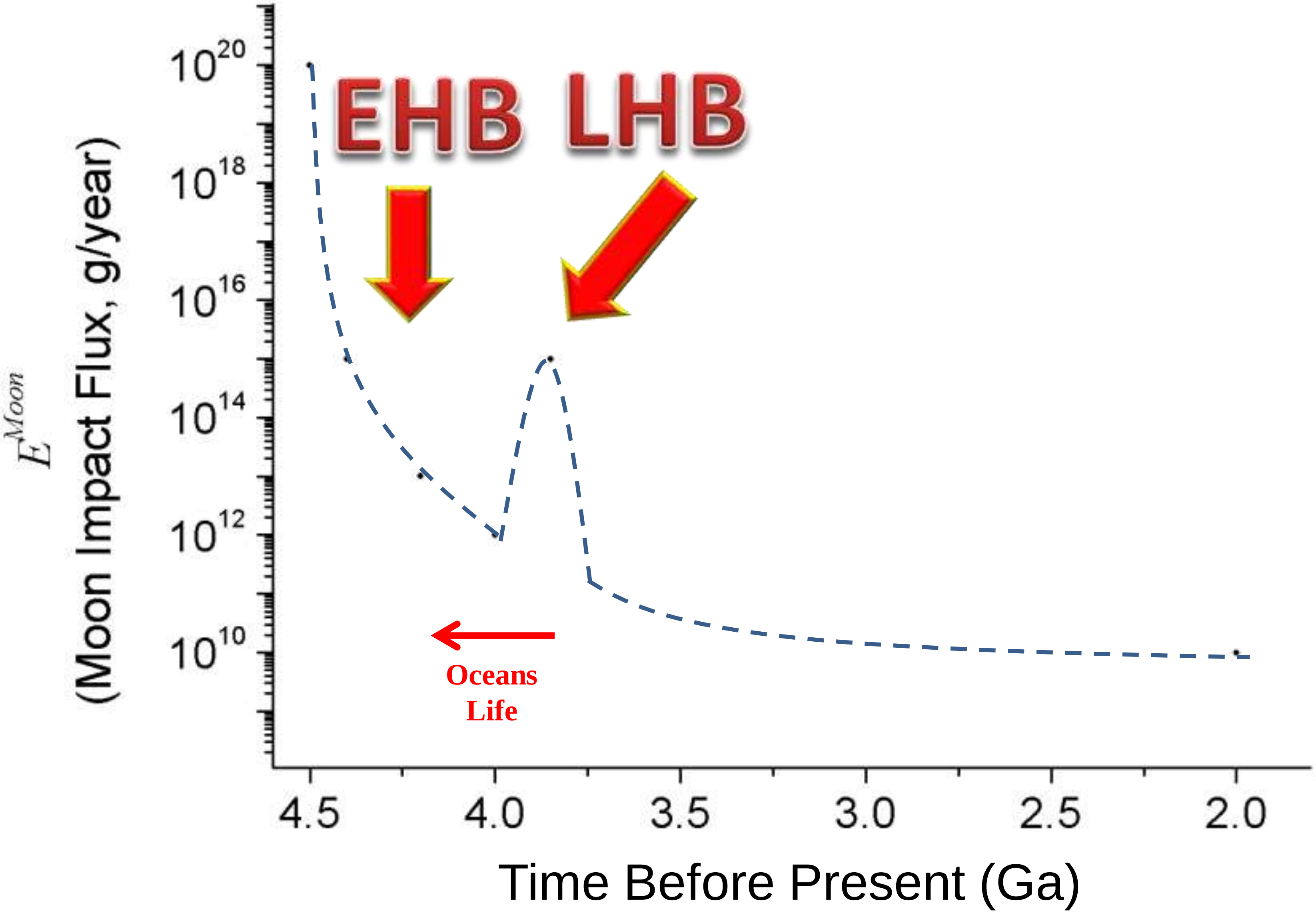

Planetary orbits and disk particle positions in the Nice model.

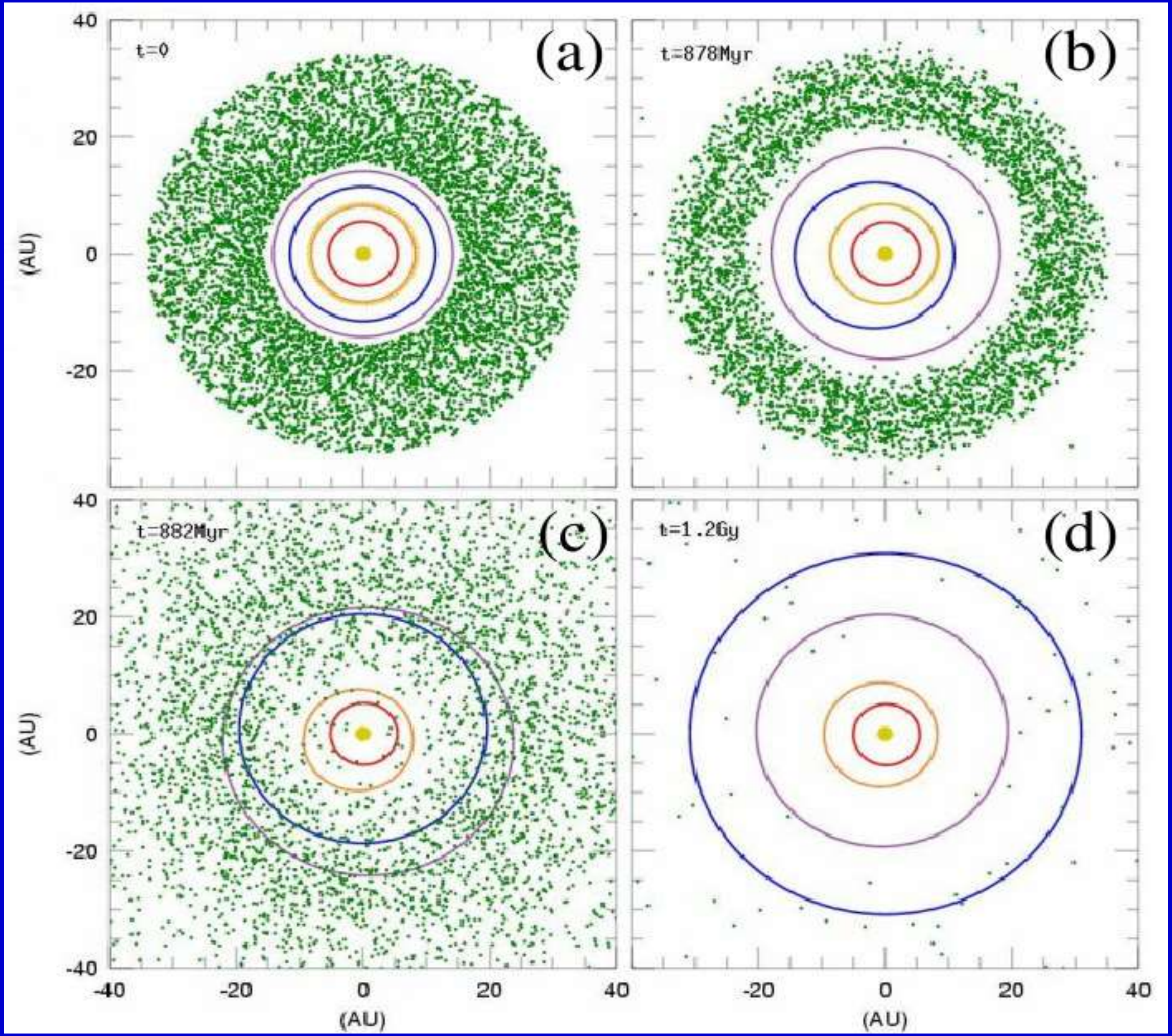

Nesvorny D, Morbidelli, A (2012) STATISTICAL STUDY OF THE EARLY SOLAR SYSTEM'S INSTABILITY WITH FOUR, FIVE, AND S SIX GIANT PLANETS, *Astron J* , 144.

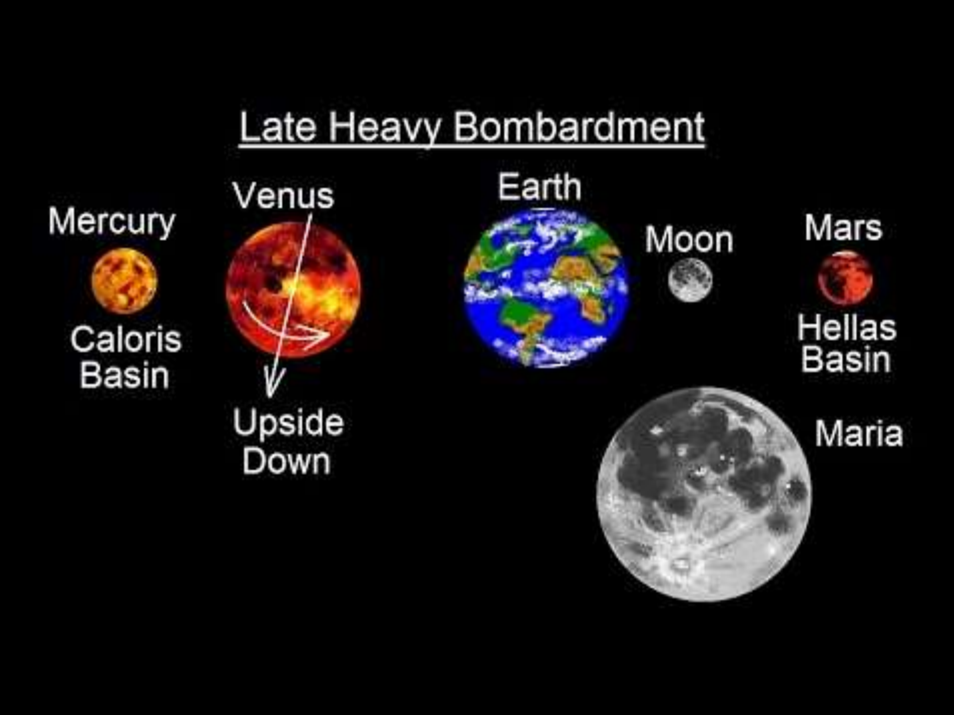
Late Heavy Bombardment
Mercury
Caloris Basin
Venus
Upside Down
Earth
Moon
Mars
Hellas Basin
Maria

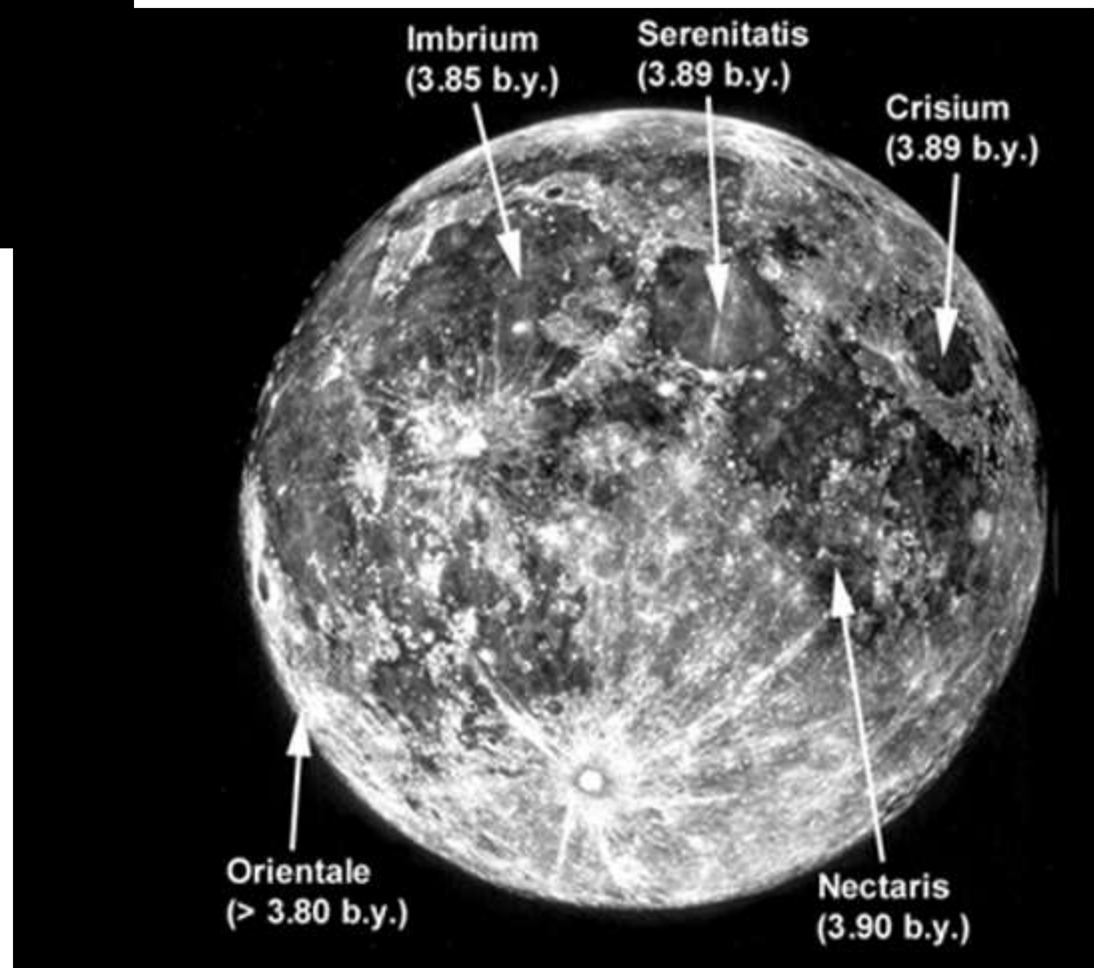
Imbrium (3.85 b.y.)
Serenitatis (3.89 b.y.)
Crisium (3.89 b.y.)
Orientale (> 3.80 b.y.)
Nectaris (3.90 b.y.)


Research on Chemical Consequences
Of High Density Energy Event
Organics
CO_2 CO
H_2O
HCN, NH_3

High Power Lasers

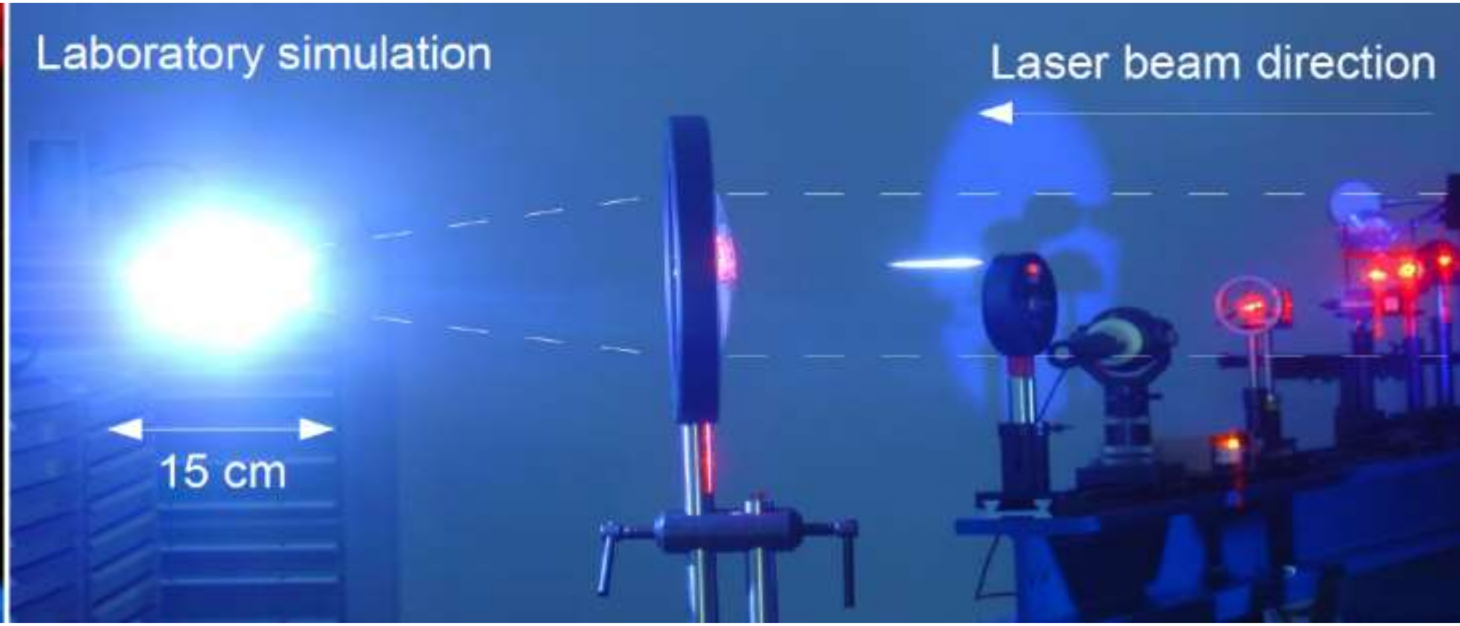

High Power Laser Mimics an Impact Plasma

Chemical Laser (C_3F_7 + Ar), λ = 1315 nm, E = 1 kJ / 0.5 ns
2 ml $HCONH_2$ + Nitrogen, Irradiated by 15 Pulses

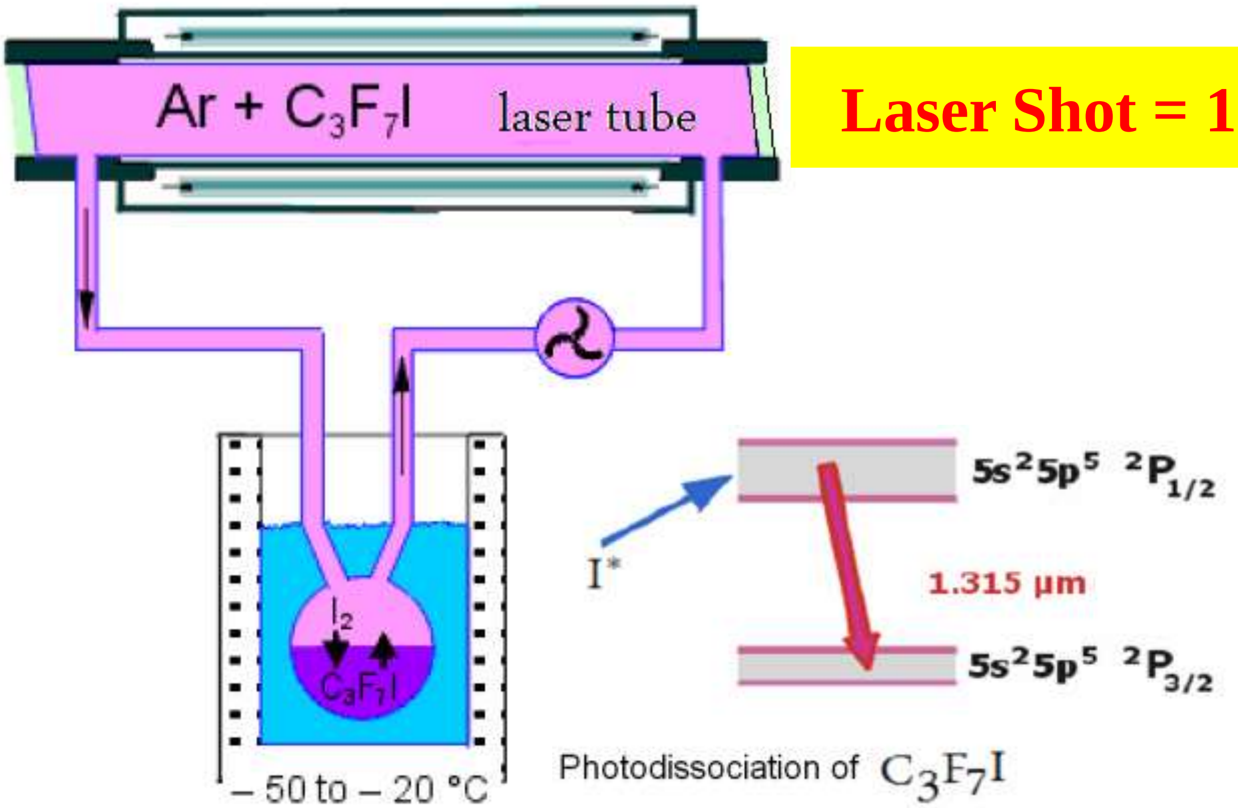

Laser Shot = 150 J

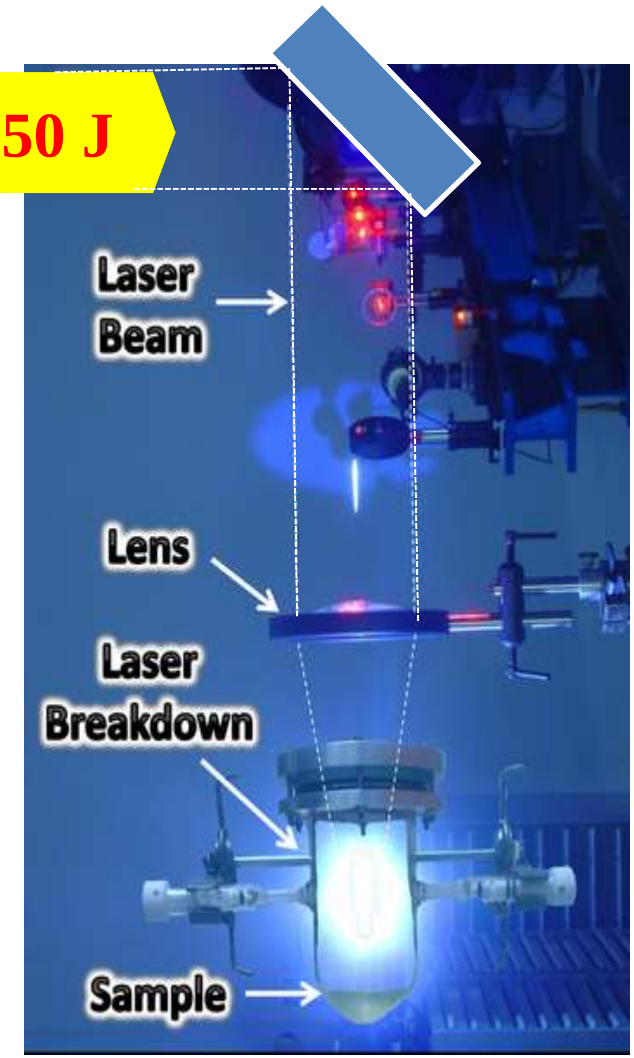

Monitorig of Stable Molecules

Ferus M, Civis S et al. (2012) *J . Am Chem Soc* 134:20788–20796

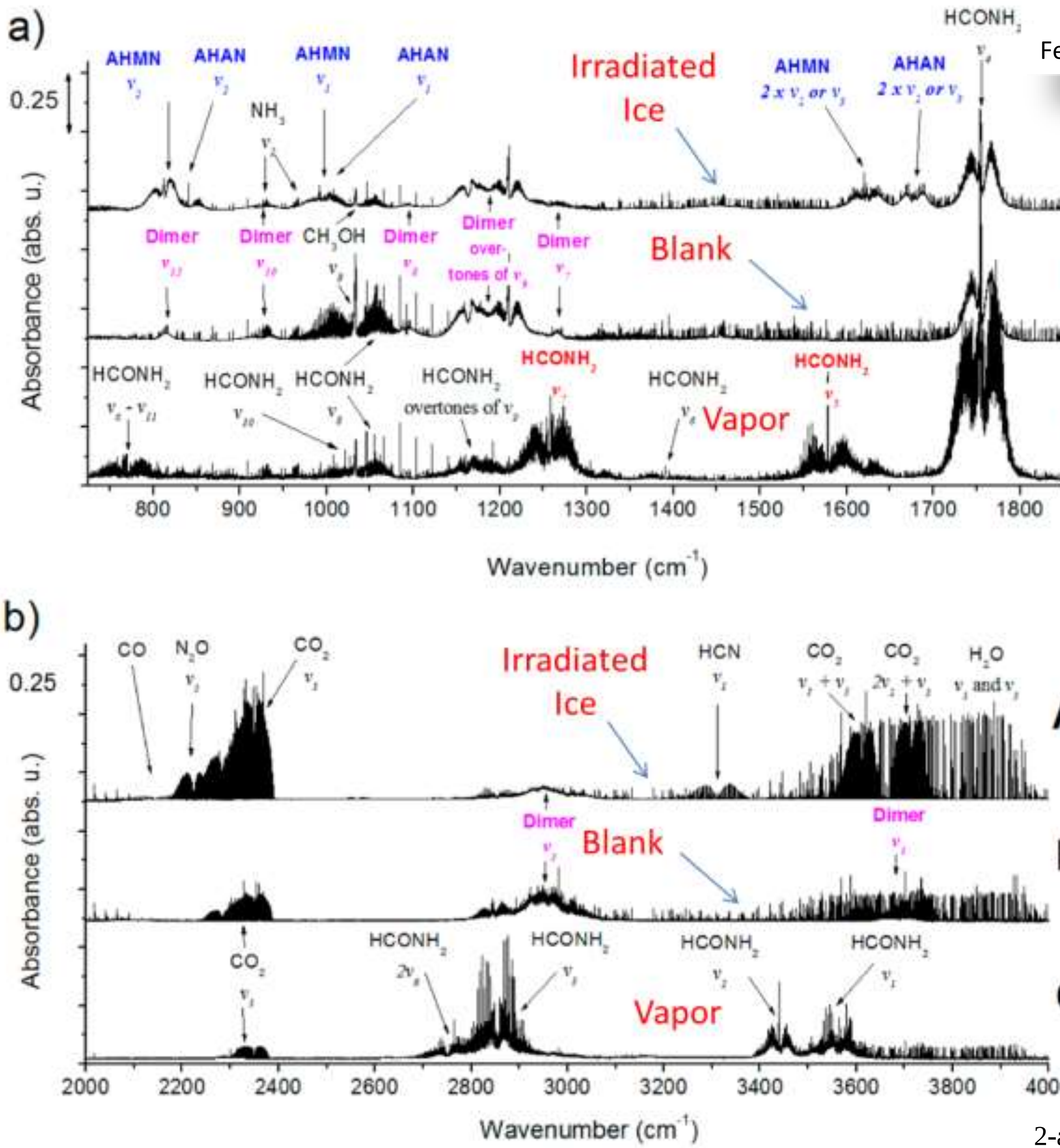

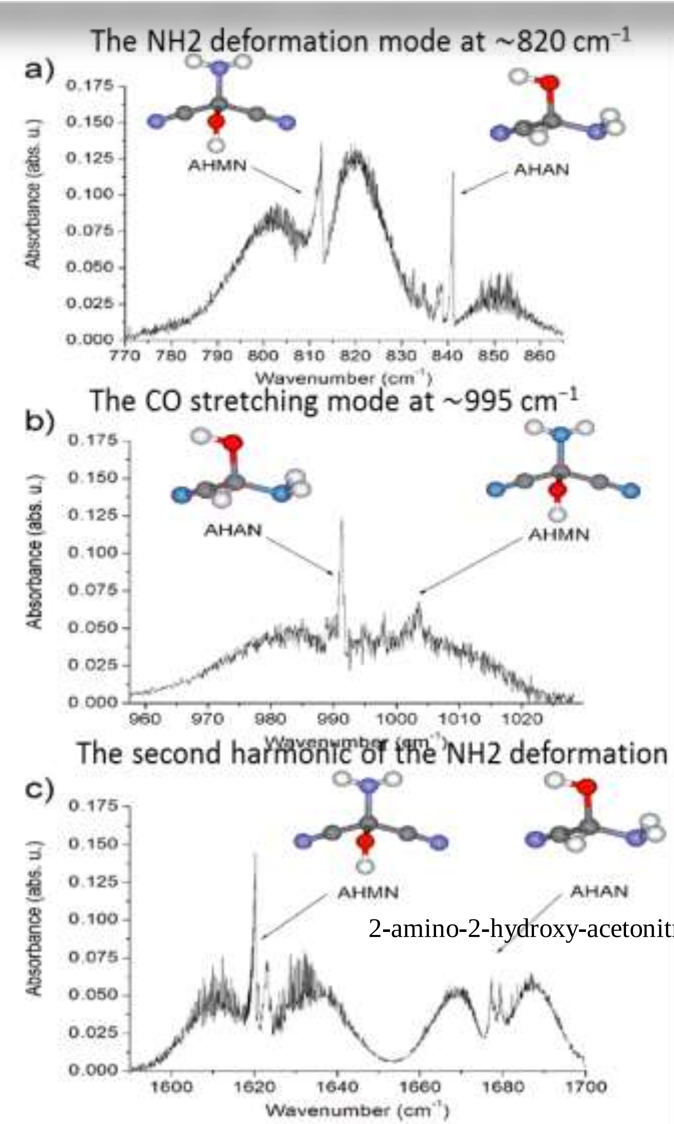

2-amino-2-hydroxy-acetonitri

2-amino-2-hydroxymalononitrile

Monitoring of Unstable Radical Species

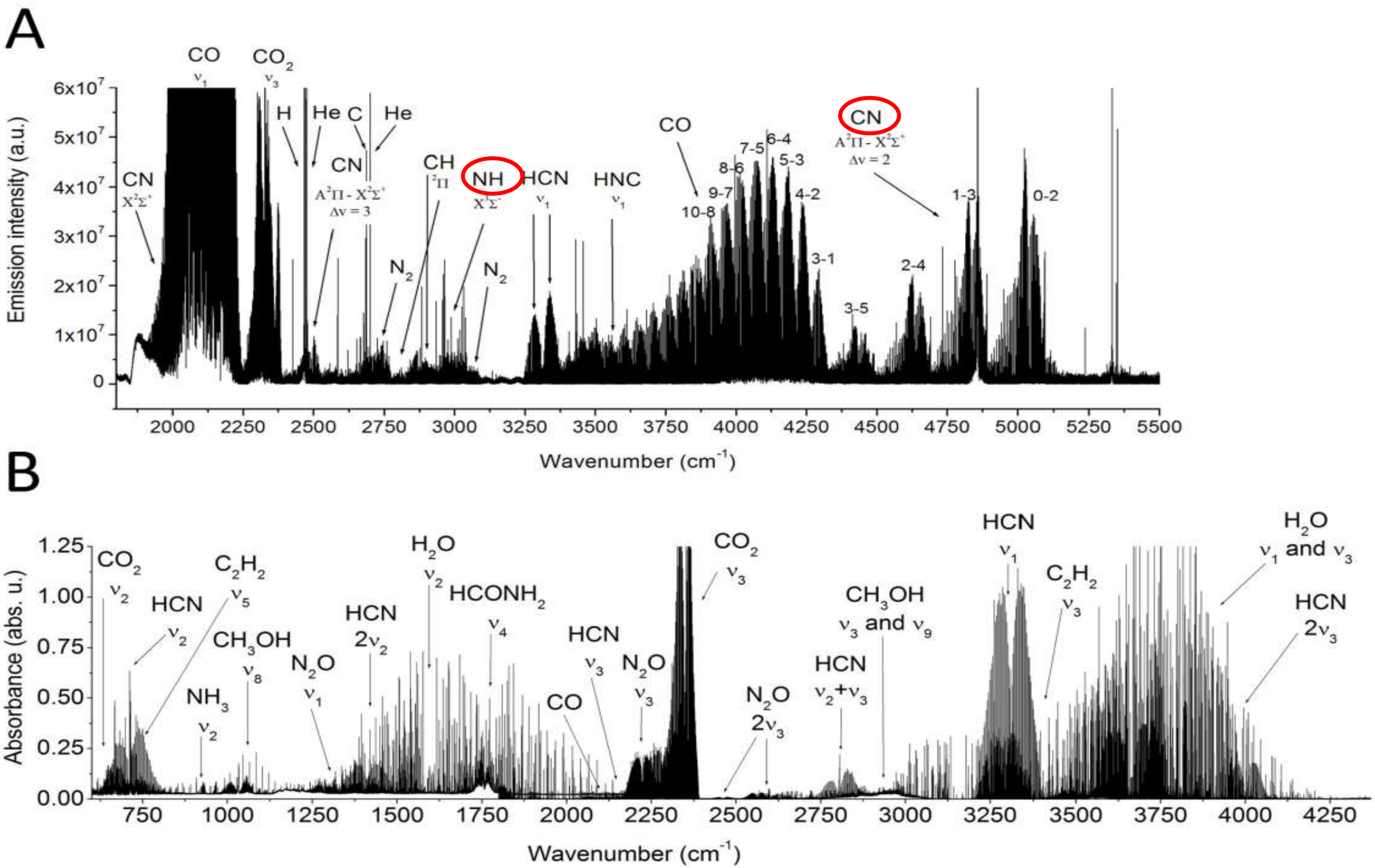

Model of Plasma Chemistry

Ferus M , Civis S et al. (2014)
J Phys Chem 118:719–736.

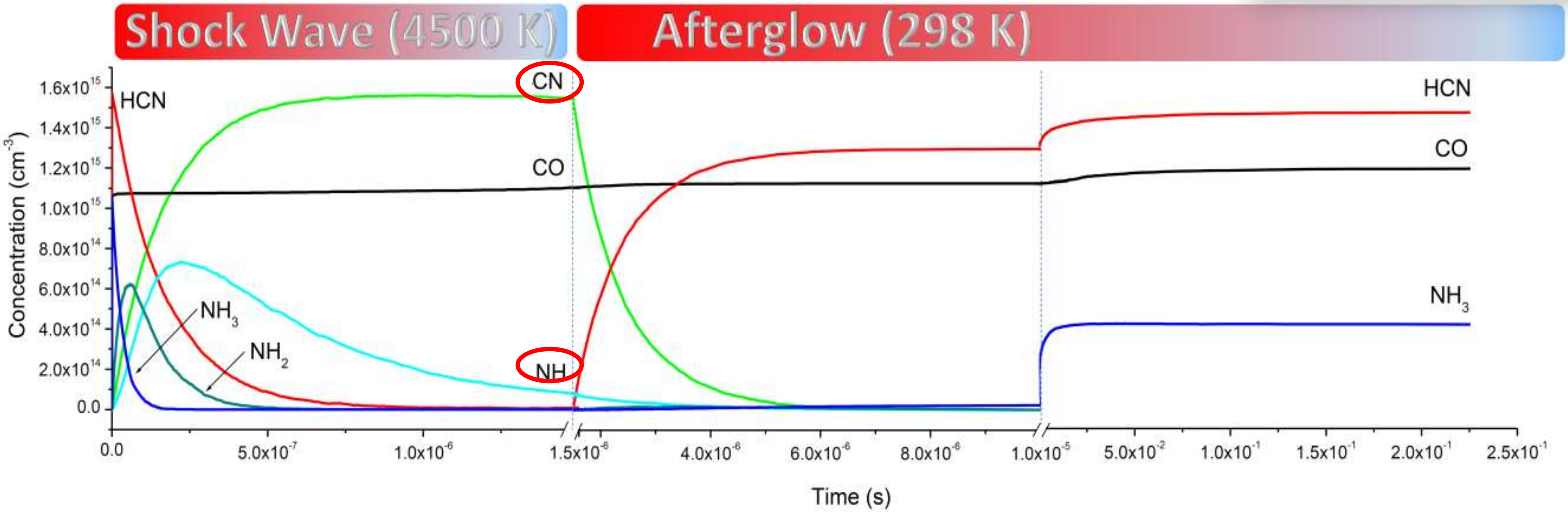

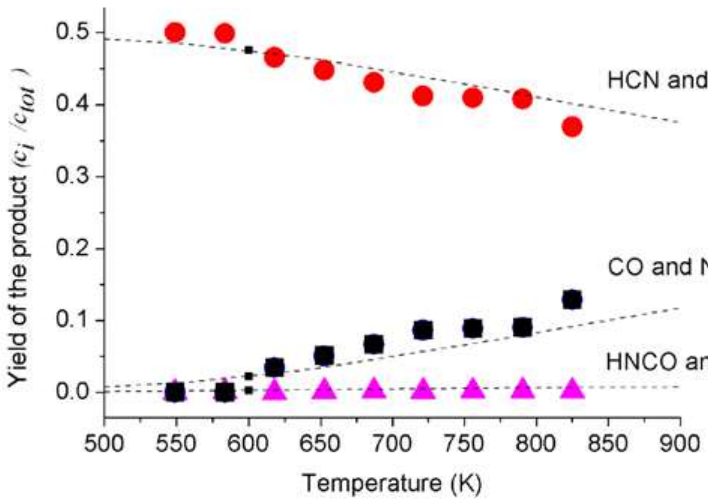

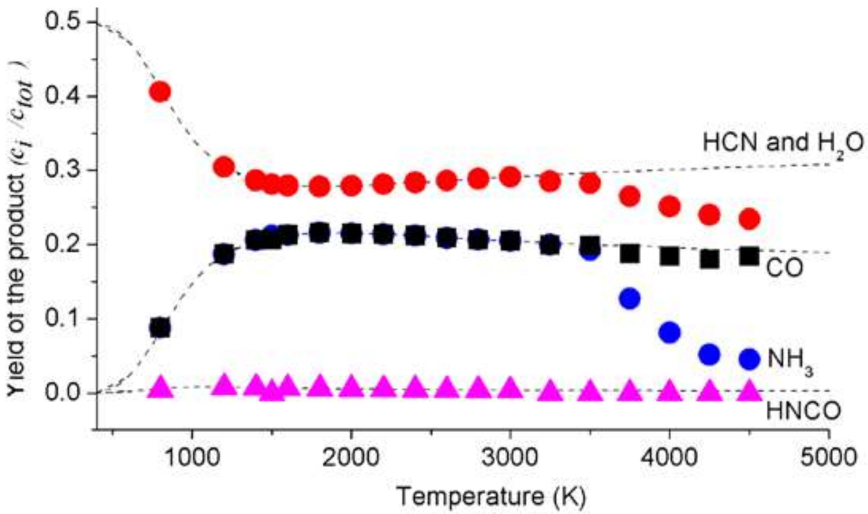

Biomolecules Detection

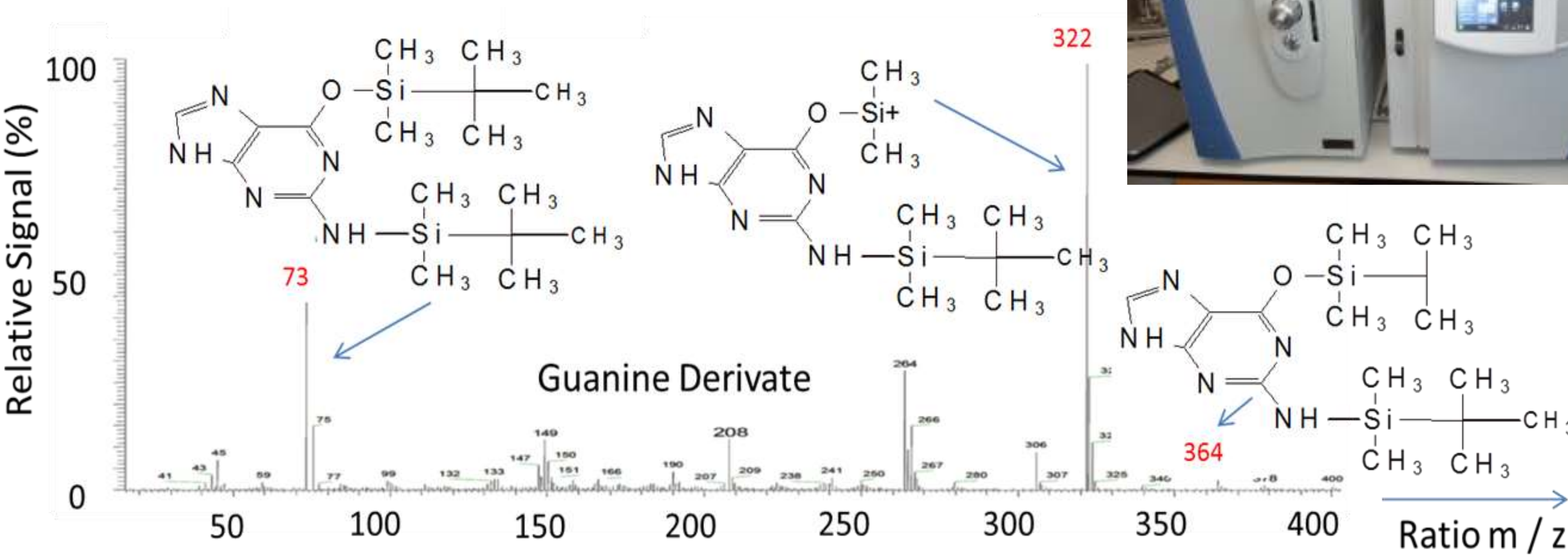

Ferus M , Civis S, Šponerová J et al. (2015)
PNAS 112:657–662.

Experiment	Adenine, %	Guanine, %	Cytosine, %	Uracil, %	Yield, mg/L
$HCONH_2$	61.9	24.0	0.0	14.1	3.71
$HCONH_2$ + chondrite	54.5	33.0	0.0	12.5	3.51
$HCONH_2$ + clay	79.4	4.4	13.1	3.1	47.07
DAMN	7.8	4.5	86.0	1.8	24.74

Chemical Model – Formation of Nucleic Bases

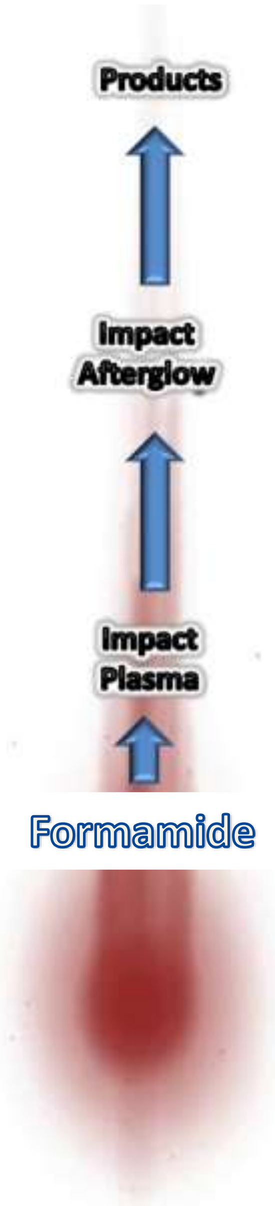

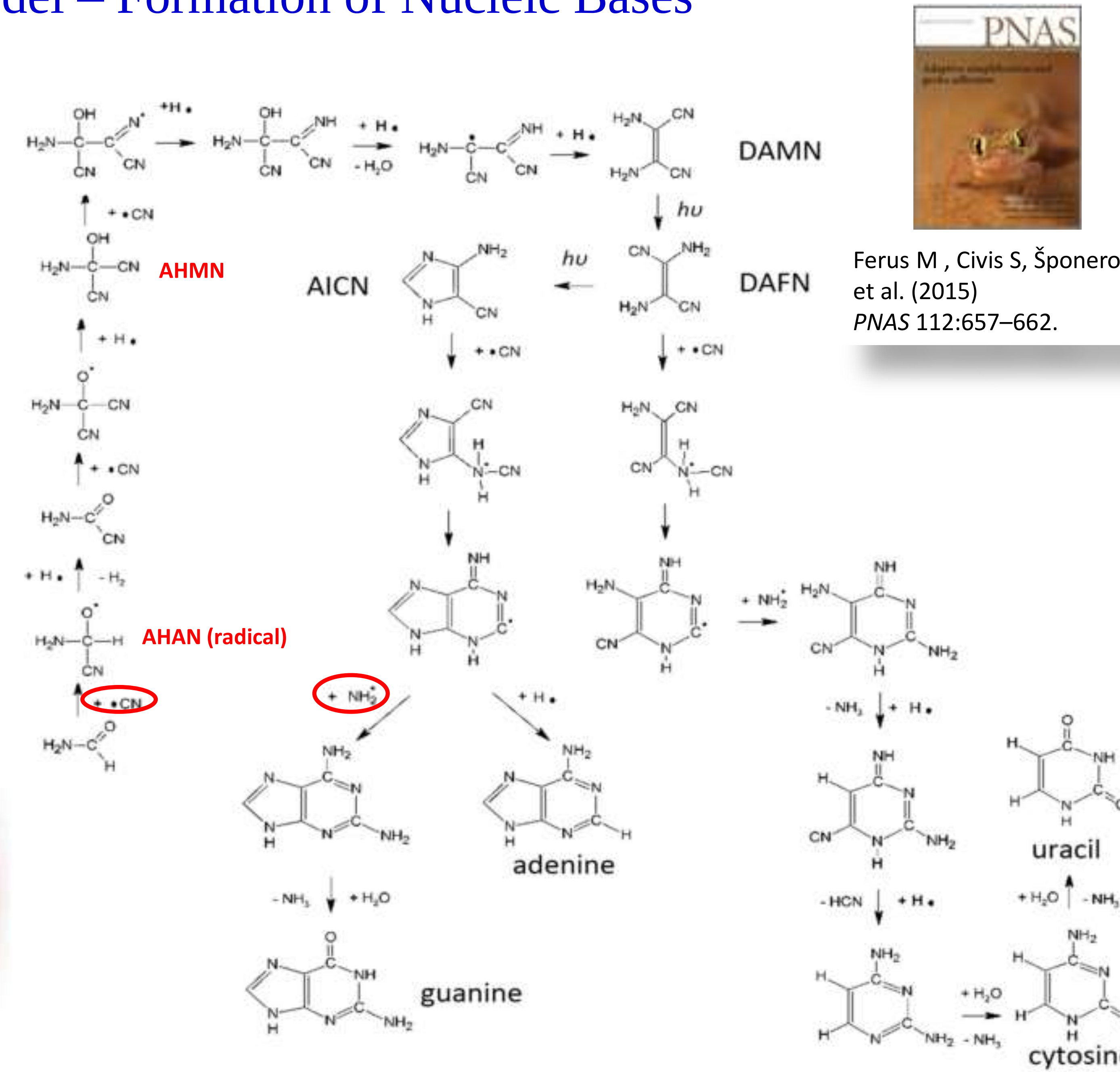

Ferus M , Civis S, Šponerová J et al. (2015)
PNAS 112:657–662.

Recent observation – Formation of Sugars

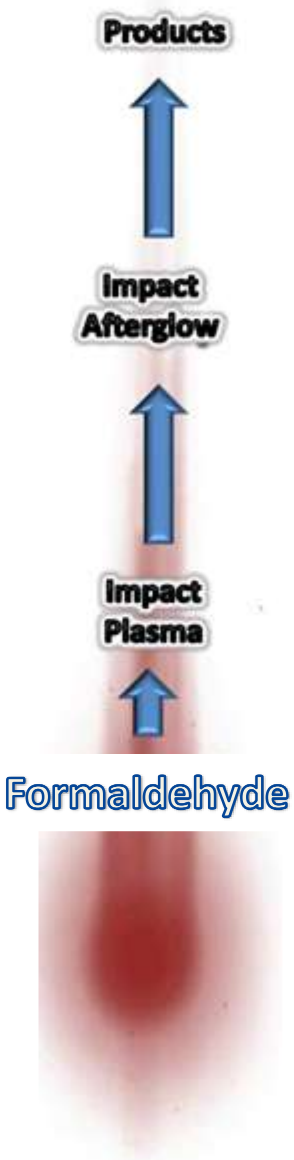

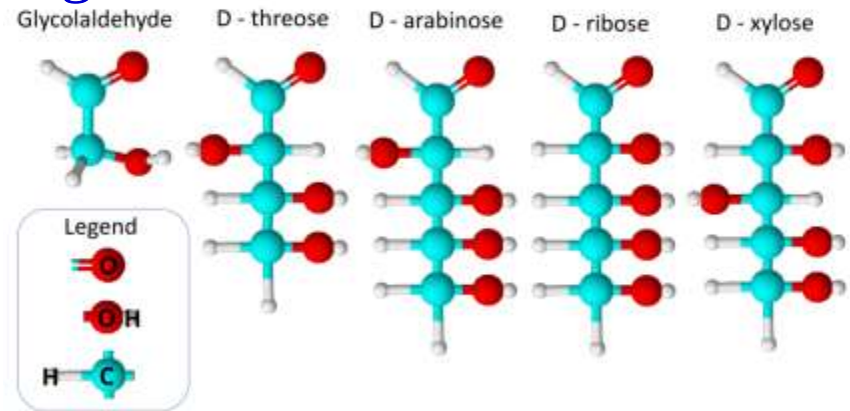

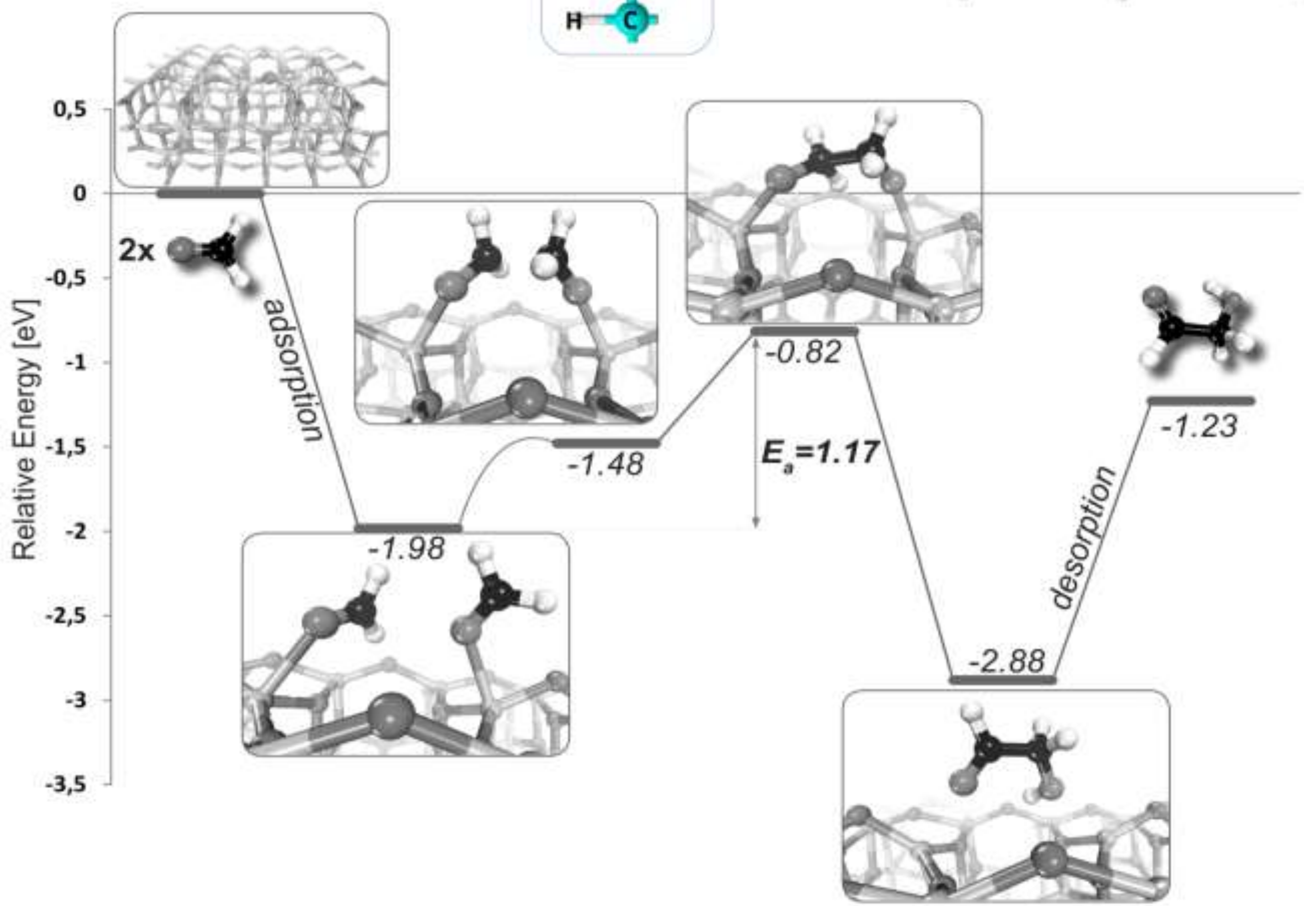

High-energy chemistry of formamide: A unified mechanism of nucleobase formation

artin Ferus[a,b], David Nesvorný[c], Jiří Šponer[b,d], Petr Kubelík[a], Regina Michalčíková[a], Violetta Shestivská[a],
dit E. Šponer[b,d,1], and Svatopluk Civiš[a,1]

Heyrovský Institute of Physical Chemistry, Academy of Sciences of the Czech Republic, 182 23 Prague 8, Czech Republic; [b]Institute of Biophysics, Academy Sciences of the Czech Republic, 612 65 Brno, Czech Republic; [c]Department of Space Studies, Southwest Research Institute, Boulder, CO 80302; d [d]Central European Institute of Technology, Masaryk University, 625 00 Brno, Czech Republic

is Feature Article is part of a series identified by the Editorial Board as reporting findings of exceptional significance.

ited by Jerrold Meinwald, Cornell University, Ithaca, NY, and approved November 4, 2014 (received for review July 2, 2014)

e coincidence of the Late Heavy Bombardment (LHB) period and e emergence of terrestrial life about 4 billion years ago suggest at extraterrestrial impacts could contribute to the synthesis of the ilding blocks of the first life-giving molecules. We simulated e high-energy synthesis of nucleobases from formamide during e impact of an extraterrestrial body. A high-power laser has en used to induce the dielectric breakdown of the plasma oduced by the impact. The results demonstrate that the initial sociation of the formamide molecule could produce a large nount of highly reactive CN and NH radicals, which could further act with formamide to produce adenine, guanine, cytosine, and acil. Based on GC-MS, high-resolution FTIR spectroscopic results, well as theoretical calculations, we present a comprehensive echanistic model, which accounts for all steps taking place in the udied impact chemistry. Our findings thus demonstrate that traterrestrial impacts, which were one order of magnitude more undant during the LHB period than before and after, could not only stroy the existing ancient life forms, but could also contribute to e creation of biogenic molecules.

gin of life | asteroid impact | biomolecules | LIDB

As the Sun formed from its molecular cloud, it was accompanied by a disk of material that consisted of gas and small st particles. Over several tens of millions of years, these dust rticles accumulated and formed the planets we see today. This ocess occurred in several stages in the terrestrial planet zone, entually culminating in massive, potentially moon-forming pacts on the proto-Earth (1). Then, following the solidification the Moon ~4.5 Ga, the initially heavy impactor flux declined) and increased again during the Late Heavy Bombardment HB) some ~4–3.85 Ga (2). Our best models for the origin of e LHB link the LHB to a dynamic instability in the outer solar stem (the so-called Nice model) (3, 4), when Jupiter's orbit anged as a result of close encounters with ice giants and small ometary bodies. These changes resulted in the release of pactors from their previously stable asteroidal and cometary servoirs. The synthesis of observation and theoretical conaints indicates that the impactor flux on Earth was ~10 times gher at the LHB than in the period immediately preceding the HB and that this flux slowly decayed afterward (5–7). At the ak, the LHB most likely involved an impact frequency of 10^9 ns of material per year (ref. 5 and Fig. 1A). The typical impact eeds are estimated to have increased from ~9 to ~21 km/s ce the LHB began. The ratio of the gravitational cross-sections Earth and the Moon is found to be ~17:1. Thus, for every nar basin, such as Orientale or Imbrium, ~17 basins should ve formed on Earth (8).

Such huge impact activity also had extensive implications for e evolution of early Earth (selected milestones in early arth's history are shown in Fig. 1B) (9): The atmosphere was rtly eroded and transformed (10, 11), and the hydrosphere s enriched by water (12, 13). Crucially, these impact-related processes most likely also contributed to the transformation of biomolecules and their precursors on Earth's surface, which would have relevant consequences on the origin of life (14, 15).

Although the impact energies were most likely not large enough to produce ocean evaporation or globally sterilizing events (16), they could have served as local energy sources for biomolecule synthesis (17–19) Therefore, the high-impact activity may not have been harmful for the formation of biomolecules and the first living structures. Conversely, it may have been the source of energy required to initiate chemical reactions, such as the synthesis of biomolecules (20).

One of the current landmarks of prebiotic chemistry is the proposal that formamide could be the parent compound of the components of the first informational polymers (21). Saladino et al. extensively studied the formamide-based chemistry that can lead to the synthesis of nucleobases and nucleotides and their metabolic products (22–24). By choosing the appropriate catalyst, purine, adenine, guanine, and cytosine (catalyzed by limestone, kaolin, silica, alumina, or zeolite), thymine (irradiated by sunlight and catalyzed by TiO_2), and hypoxanthine and uracil (in the presence of montmorillonites) were obtained (23–27).

Our recent studies reported the formation of the canonical nucleobases, as well as purine and glycine, during the dielectric breakdown induced by the high-power laser Asterix in the presence of catalytic materials (meteorites, TiO_2, clay) (17, 18). Formamide-based synthesis in the high-density energy event (impact plasma) can solve the long-standing enigma of the simultaneous formation of all four nucleobases. The main objective of the present study is to demonstrate a unified mechanism of the formation of the nucleobases through the reaction of formamide and its dissociation products in a high-energy impact event relevant to LHB.

Significance

This paper addresses one of the central problems of the origin of life research, i.e., the scenario suggesting extraterrestrial impact as the source of biogenic molecules. Likewise, the results might be relevant in the search of biogenic molecules in the universe. The work is therefore highly actual and interdisciplinary. It could be interesting for a very broad readership, from physical and organic chemists to synthetic biologists and specialists in astrobiology.

Author contributions: M.F., J.E.S., and S.C. designed research; M.F., J.S., P.K., R.M., and V.S. performed research; M.F. and J.E.S. analyzed data; and M.F., J.E.S., S.C., and D.N. wrote the paper.

The authors declare no conflict of interest.

This article is a PNAS Direct Submission.

[1]To whom correspondence may be addressed. Email: svatopluk.civis@jh-inst.cas.cz or judit@ncbr.muni.cz.

This article contains supporting information online at www.pnas.org/lookup/suppl/doi:10.1073/pnas.1412072111/-/DCSupplemental.

COMMENTARY

Impact synthesis of the RNA bases

Andro C. Rios[1]

Exobiology Branch, Space Science and Astrobiology Division, NASA Ames Research Center, Moffett Field, CA 94035

Any discussion related to how life began on this planet inevitably invokes the question as to the origin of bio-organic molecules, a field called prebiotic chemistry (1). How did organic compounds come to populate the early Earth? Before 1953, this question itself was not widely considered within the realm of experimental science. However, since the pioneering results of the Miller–Urey experiment that produced amino acids from electrical discharges passing through simple gases (2), the field of prebiotic chemistry has been extremely prodigious in demonstrating abiotic syntheses for multitudes of organic compounds. However, it became apparent that prebiotic chemistry was faced with a more challenging question. How did the biomolecules of life get selected out of such complex, prebiotic mixtures?

Particular significance has been placed on understanding the selection of the nucleobases adenine (A), cytosine (C), guanine (G), and uracil (U), given their role in the RNA world hypothesis (3). The hypothesis is a premise that life may have emerged with genetic and enzymatic function based exclusively on RNA (4). Some research has pointed to the possibility that selection criteria may have relied on nucleobases that were able to persist the longest in the prebiotic environment. Others have considered the possibility that early RNA life used a wide range of nucleobases, and over time unique selection pressures emerged that favored the extant bases. In terms of using a synthetic origin or availability argument, it has been found that varying conditions are needed to demonstrate the production of all of the RNA bases. Invoking multiple stage and multiple environmental scenarios for the selective prebiotic synthesis of the nucleobases seems extremely unlikely. What would be intriguing would be the demonstration that all of the RNA bases are selectively produced under the same conditions, and that those conditions might be considered plausible to prebiotic chemistry and the early Earth environment. This is what Ferus et al. set out to do in their most recent contribution, and they begin with a simple organic compound called formamide (Fig. 1) (5).

Formamide appears to be widespread in the universe. Astronomers have recently reported its presence in our solar system found within the atmospheres of comets (6), and since the 1970s, formamide has been detected in multiple regions in the interstellar medium (7). The known chemistry and ubiquity of formamide has made it an attractive primordial feedstock compound for the production of many prebiotic molecules (8). Experiments on the prebiotic synthesis of nucleobases using formamide have

Simulated impact or shock synthesis of organic compounds has remained a plausible model for the production of organic compounds needed for prebiotic chemistry.

been an active area of research (9–11), but some disheartening observations were routinely made. At best, only three of the four RNA bases have been observed in a single experiment. The missing base typically was guanine. However, when the prebiotic synthesis of guanine could be demonstrated, it would be at the exclusion of other bases, often a pyrimidine, such as cytosine or uracil. However, these studies were important because they demonstrated that formamide could be a common feedstock for each RNA base. What remained was the task of finding plausible conditions that could access all of the bases in one experiment (8).

In a previous publication, Ferus et al. had calculated that if formamide were exposed to much higher energies it would be able to access reaction pathways that produce the nucleobase products (12). Thus, a central model in their current work (5) is the subjection of formamide to experiments that simulate the energy output resulting from an extraterrestrial impact. Simulated impact or shock synthesis of organic compounds has remained a plausible model for the production of organic compounds needed for prebiotic chemistry and the origin of life (13, 14). A tantalizing argument for this scenario lies with the coincidence of estimates for when life might have originated (4.4–3.5 billion y ago) and the Late Heavy Bombardment (4.0–3.8 billion y ago), a period when the early Earth received a pronounced increase in the impact rate of asteroidal and cometary material (15).

Ferus et al. (5) follow the aftermath of the simulated impact, which causes the breakdown of formamide into a variety of simple gases and radical intermediates (see Fig. 1). The authors show how the formation of these radicals, mainly CN• and H•, combine with formamide to increase the molecular complexity of the mixture leading to stable and previously studied chemical intermediates. In combination with their previous work, Ferus et al. detail how the radicals CN•, H•, and NH_2•, continue to drive the chemistry to produce the purines and pyrimidines (12, 16). A unifying outcome, and of particular interest to prebiotic chemistry, is Ferus et al.'s (5) demonstration that 2, 3- diaminomaleonitrile (DAMN) is a common precursor to all of the RNA bases under these conditions. DAMN has long been known to be a key chemical precursor to the purine nucleobases (1, 9–11), but this is the first report that DAMN has been implicated in the synthesis of pyrimidines. The generation of the CN• radical from the breakdown of formamide and its subsequent reactions has been calculated to be the explanation for how DAMN can access both reaction pathways of pyrimidines and purines.

The prebiotic synthesis of nucleobases helps address only one of a long list of questions. The origin-of-life community also needs convincing reports to demonstrate how the bases could have realistically accumulated in the early Earth environment. How prebiotic organics escaped degradation by the widespread occurrence of water on the early Earth is an example of such a question. In the late 1990s, Stanley Miller and coworkers investigated the hydrolytic stabilities of nucleobases at high temperatures to

Author contributions: A.C.R. wrote the paper.

The author declares no conflict of interest.

See companion article on page 657.

[1]Email: andro.c.rios@nasa.gov.

IFS125HR

Parameters
- Spectral range: 50,000 - 5 cm^{-1}
- Ultimate resolution: < 0.001 cm-1
- Wavenumber accuracy: < 5 x 10^{-7} times wavenumber (absolute)

Design
- Vacuum system: < 2x10-2 hPa (mbar)
- Up to 3 internal source and 6 detectors

Accessories
- Gas cell (3,6 – 40m)
- Bolometer

Cena
- 13 mil. Kč bez DPH

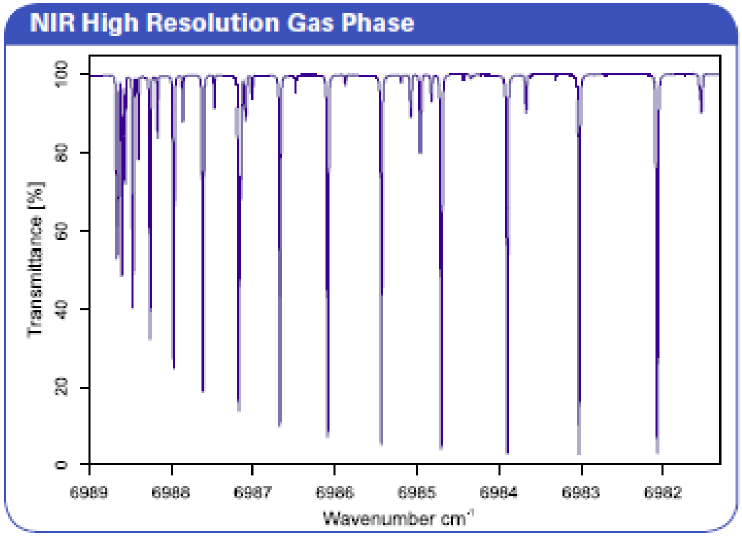

Multipath Gas Cell

Spektrograf ESA 4000-LAB

Technical specification Echelle spektrograph ESA 4000-LAB

Spectral range at simultaneous detection	200 – 780 nm or 191 – 420 nm
Linear dispersion per pixel (24 µm)	0.005 nm (200 nm) 0.010 nm (400 nm) 0.019 nm (780 nm)
Resolution with respect to one pixel (λ / $\Delta\lambda$)	40000
Diffraction orders	30 – 120 or 58 – 126
Focal length	25 cm
Aperture	1 : 10
Flat image plane	24.5 x 24.5 mm^2

ESA 4000

The Echelle spectra analyzer ESA 4000 is a compact spectrograph for simultaneous detection of complex spectra within the UV/VIS range. It consists of the Echelle spectrograph and the electronic control unit for camera control and synchronisation of data acquisition with external devices like a pulsed laser system.

Echelle spectrograph

The tetrahedral mounting of the Echelle spectrograph is characterized by a simple, but effective aberration correction of the whole optical system. The Echelle grating generates up to hundred overlapping diffraction orders separated by the quartz prism in front of the grating as a two-dimensional pattern. Thus the compact spectrograph covers a total spectrum length of over one meter on a one square inch focal plane. A high spectral resolution and simultaneous broad spectral range detection of nearly all analytical lines of interest and their spectral background are achieved.

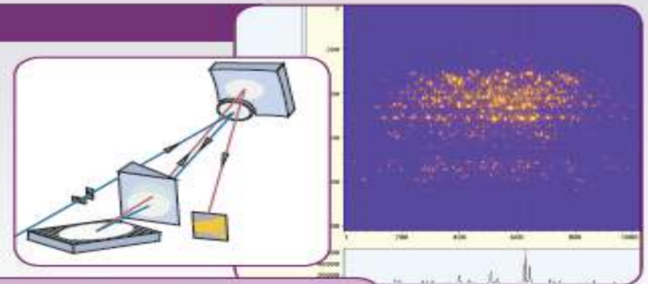

Simultaneous detection within the UV - VIS range
Ultra high spectral resolution
Gateable image intensifier
Compact design for systems integration

ICCD camera

The CCD-camera detector head is integrated in the spectrograph to ensure proper operation also in a rough environment. It is equipped with a gated MCP-image intensifier for measurement of very weak light sources as well as for short light pulses.
The analog signal processing uses a circuitry with time correlated double sampling.
Subtracting the dark current signal from the spectral signal minimizes the noise of the detector output stage.
Uninteresting spectral ranges may be summarized and removed to increase data processing speed (hardware binning).

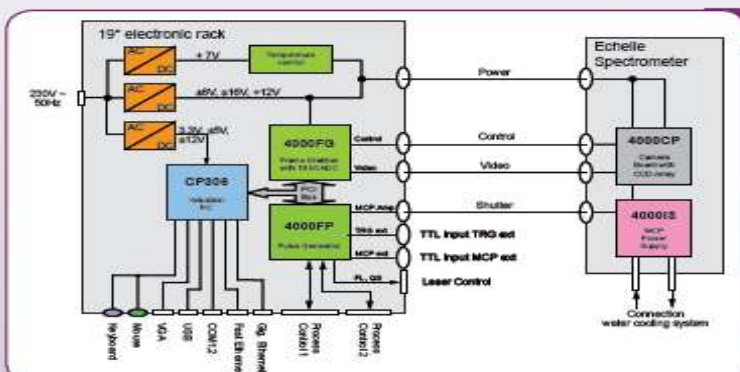

Electronic control unit

The 19"-electronic-rack includes power supplies for the camera, the frame grabber board with a 16 bit ADC, an industrial PC and interfaces.
The integrated fast pulse generator board is developed for time resolved measurements and can be triggered internally or externally. In case of internal triggering the generator board allows controlling measurements with a time resolution of 20 ns.
Additional control pulses are available for external triggering of pulsed light sources.

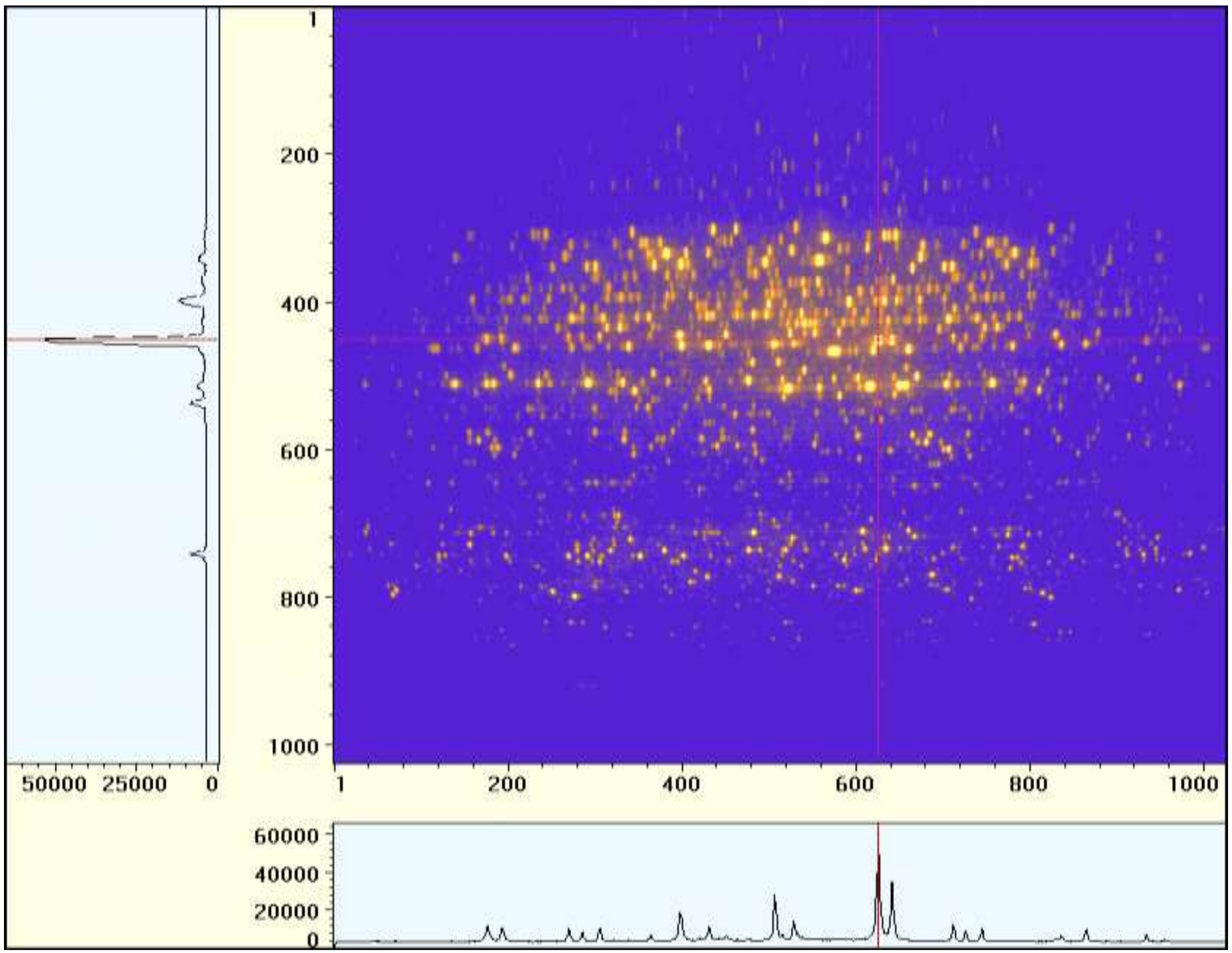

1
200
400
600
800
1000
50000
25000
0
1
200
400
600
800
1000
60000
40000
20000
0

Applications

The Echelle system covers almost every application in atomic spectroscopy.

Atomic emission spectroscopy

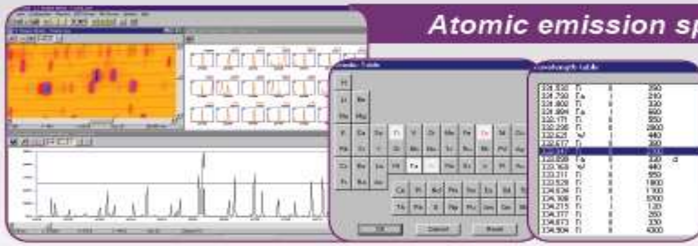

Laser induced emission spectrum of tool steel
Data visualisation via ESAWIN software - camera picture, calculated wavelengths spectrum, selection of analysis lines and element classification

The broad spectral range detection combined with a high spectral resolution ensures a simultaneous multi-element analysis of almost every chemical element. Measurements of steel confirm the high quality of the spectra.
In spite of the extremely large number of iron lines, a largely undisturbed spectral line structure is visible.

Molecular spectroscopy

Echelle picture and wavelengths spectrum of a CN-molecular emission - violet bands system
Laser induced emission spectrum of a wood sample in air

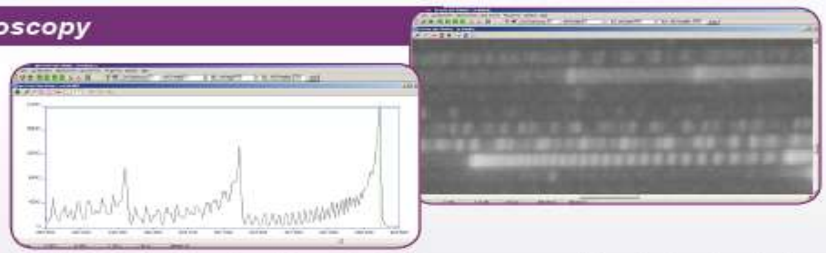

The high spectral resolution enables investigations of reaction products in plasma processes like radicals and molecules. Additionally to the excited atomic lines, molecular bands were monitored during plasma generation by laser ablation. The pictures show time-resolved measurements of CN-emission bands which occur in case of vaporization of carbon containing samples in air.

Absorption spectroscopy

Measurement of air absorption in the UV range
Echelle picture and spectral detail of the O_2 absorption bands below 200 nm
Light source: deuterium lamp

The combination of the ESA 4000 with a wide band light source permits the simultaneous measurement of broad range absorption spectra. Real-time monitoring of atmospheric impurities (aerosols) is a practical application. The example demonstrates the fine spectral features of O_2 absorption bands in the UV spectral region marking the end of the measurement range in air.

Technical specification

Spectrograph	
Echelle optics	
Spectral range at simultaneous detection	200 - 780 nm or 191 - 420 nm
Linear dispersion per pixel (24 µm)	0.005 nm (200 nm), 0.010 nm (400 nm), 0.019 nm (780 nm)
Resolution with respect to one pixel ($\lambda / \Delta\lambda$)	40000
Diffraction orders	30 - 120 or 58 - 126
Focal length	25 cm
Aperture	1 : 10
Flat image plane	24.5 x 24.5 mm²
Entrance slit	Single fiber input, SMA connector
Camera	Integrated, with closed water cooling system
Size	300 x 200 x 500 mm (482 x 258 x 585 mm OEM version)
Weight	13 kg (15 kg OEM version)

ICCD camera	
CCD	Kodak KAF-1001 frame transfer CCD (1024 x 1024 pixels)
	Pixel size 24 x 24 µm
	TE stabilization of temperature
	Programmable line binning (on-chip)
Image intensifier	Proxitronic image intensifier with microchannel plate
	UV enhanced S20 photocathode
	Fiber optic coupling to CCD
	Gateable from 20 ns to 16 s

Electronic control unit	
Frame grabber board	Readout rate selectable 0.5, 1, 2 or 4 MHz
	16 bit ADC, 2 MB memory, PCI bus with 90 MByte/s
	Line and pixel binning
Fast pulse generator board	Repetition rate up to 200 Hz
	4 channels adjustable in steps of 10 ns
Industrial-PC	CPU CP306 Intel Pentium M, 1.86 GHz, 1 GB RAM
Interfaces	6 x USB 2.0, 2 x BNC for external triggering, process control
	Keyboard, RS 232 serial, VGA, Fast / Gigabit Ethernet
Periphery	Hard disk min. 80 GB, DVD-R/RW, power supplies
Cooling unit	Integrated water-to-air cooled heat exchanger, pump unit
Power requirements	110 / 220 / 230 V~, 50 / 60 Hz, 4 / 2 A
Operating environment conditions	Temperature 10 - 30 °C, relative humidity 20 - 80 %
Camera	Integrated, with closed water cooling system
Size	560 x 220 x 420 mm (482 x 180 x 350 mm OEM version)
Weight	21 kg (14 kg OEM version)

Software	
ESAWIN	Executable on Windows XP
	Automatic hardware control of all measuring parameters
	Control of external light sources like pulsed laser systems
	Analysis of data, spectral line recognition tools
	Atomic line data base
	Dialogue controlled qualitative and quantitative analysis
	Special tools for LIBS measurements
	Plasma temperature calculation
	Remote control mode

PP-MG-ESA4000-1202
Product photos by Meyerfoto

LLA Instruments GmbH
Justus-von-Liebig-Str. 9 12489 Berlin
www.lla-instruments.com mail@lla.de
Tel.: +49 30 6290790-0
Fax: +49 30 6290790-10

LLA Instruments GmbH

Process Analytical Equipment
Chemical Imaging of Material Streams

LLA Instruments GmbH, Justus-von-Liebig-Str. 9/11, 12489 Berlin, Germany

J. Heyrovsky Institute of Physical Chemistry
of the ASCR, v. v. i.
Prof. Svatopluk Civis
Dolejškova 2155/3

18223 PRAGUE 8
CZECH REPUBLIC

Quotation

Number	
Document No.	2014-12680
Date	03.03.2014
Customer No.	356

Please quote on further inquiry !

Reference		Kind of Dispatch		Contact	Olaf Krenz
Order	Inquiry	Terms of Delivery	ex works	Phone	030 6290790-46, -48
Date	26.02.2014	Your VAT-No		E-mail	o.krenz@lla.de

Sir,

Thank you for your inquiry. We are pleased to offer you the following:

Item	Article No	Description	Quantity	Unit	Price	Total Amount
1	92100020	Echelle Spectra Analyzer ESA 4000-LAB Echelle-spectrograph with ICCD camera for a wavelength range of 200 to 780 nm MCP-intensifier and fiber plate coupling with CCD detector array KAF 1001, fiber optical input, SMA-connector, standard UV fiber cable 1.5 m long Control unit: 19" electronic chassis with power supply, Industrial PC with Intel Core2LV 2,26 GHz, Fast pulse delay generator, Frame grabber with 16 bit ADC and selectable readout rate up to 4 MHz, DVD-R/RW, Keyboard and Mouse Interfaces: RS232, Fast / Gigabit Ethernet, VGA, 5 x USB, 10-pin process control connector, Laser Sync output Power supply: 230 V / 50 Hz ***consisting of*** 41030130 LCD-Monitor 19" TFT 1280 x 1024 Pixel — 1 pcs	1	pcs	53.004,00	53.004,00
2	94200020	ESAWIN Software - Software for system control - Software for spectra processing	1	pcs	3.780,00	3.780,00
3	60120004	Aluminium box Adapted box for the device.	1	pcs	1.039,50	1.039,50
4	60500001	Installation and instruction of ESA 4000 by LLA staff, one day at final customer's site including travel expenses for LLA staff	1	P	1.890,00	1.890,00
	Subtotal				59.713,50	59.713,50
				minus	10,00 %	-5.971,35

Balance to next page 53.742,15

IR astronomy facilities: space-born IR spectrographs for investigating objects other than the Sun

- Spitzer Space Telescope: resolution of $R \sim 600$ in the $\lambda = 10$–37 μ range
- AKARI satellite: Far-Infrared Surveyor (FTS with resolution $\Delta\nu = 0.19\ \mathrm{cm}^{-1}$) and a near- and mid-IR camera with a resolution of up to $\Delta\lambda = 0.0097$ μ ($R \sim 100$–1000).
- Airborne Stratospheric Observatory for Infrared Astronomy (SOFIA): Echelon-cross-Echelle Spectrograph (EXES) with a resolution of $R \sim 10^5$ in the 4.5–28.3 μ range
- Space Infrared telescope for Cosmology and Astrophysics (SPICA): mid-IR high resolution spectrometer (MIRHES) with a spectral resolution of $R \sim 3 \times 10^4$ in the 4–18 μ range

Sketch of the experimental setup

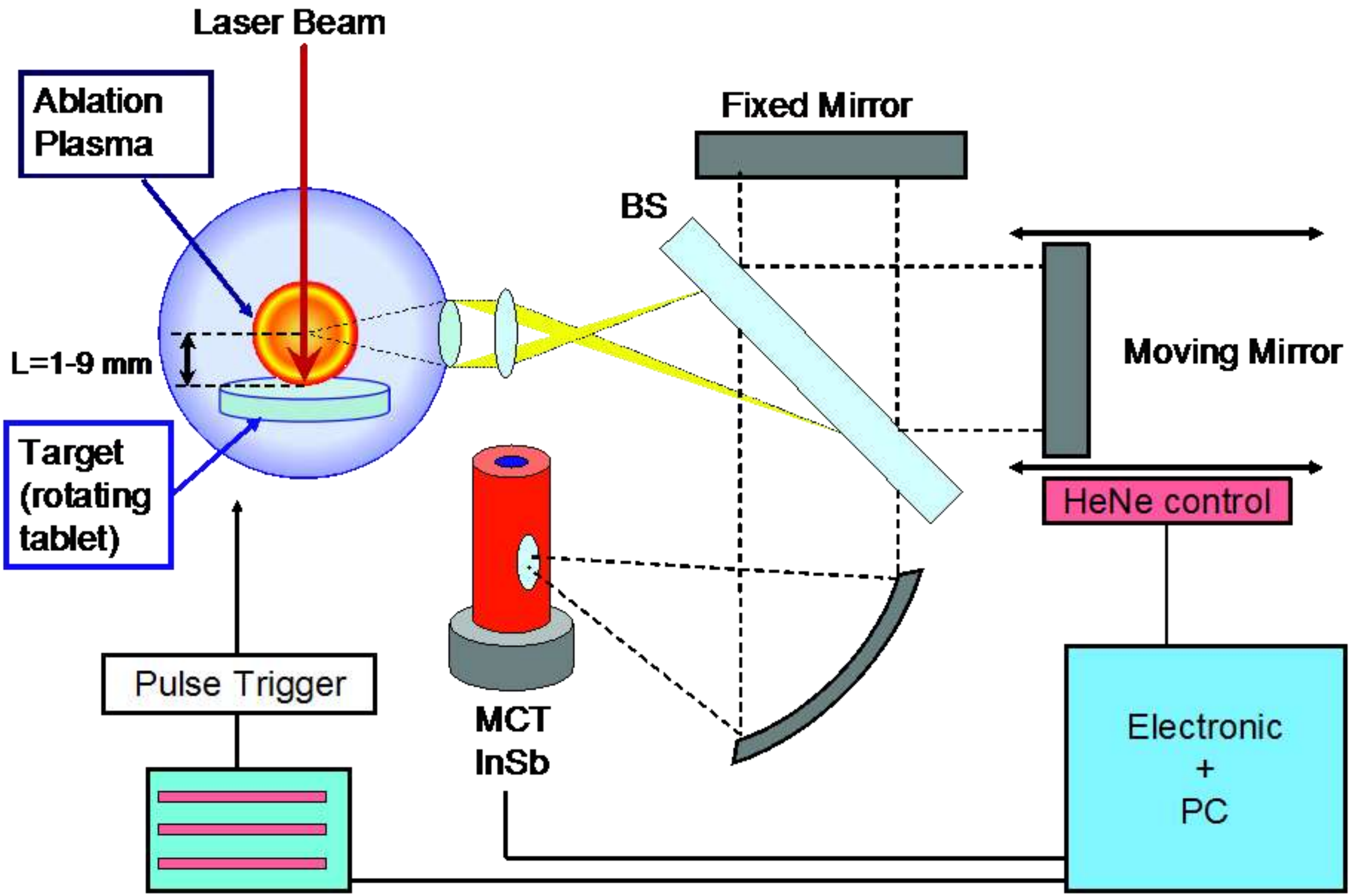

The setup parameters

- A high repetition rate ArF laser ExciStar S-Industrial V2.0 1000 (λ=193 nm) laser pulse width 12 ns, frequency 1 kHz) with 15 mJ pulse energy
- Bruker IFS 120 HR spectrometer, resolution 0.02 cm^{-1}
- Overall spectrum range: 800-7000 cm^{-1}

Dependence of the time profile on the distance *L* between the probed area and the target surface

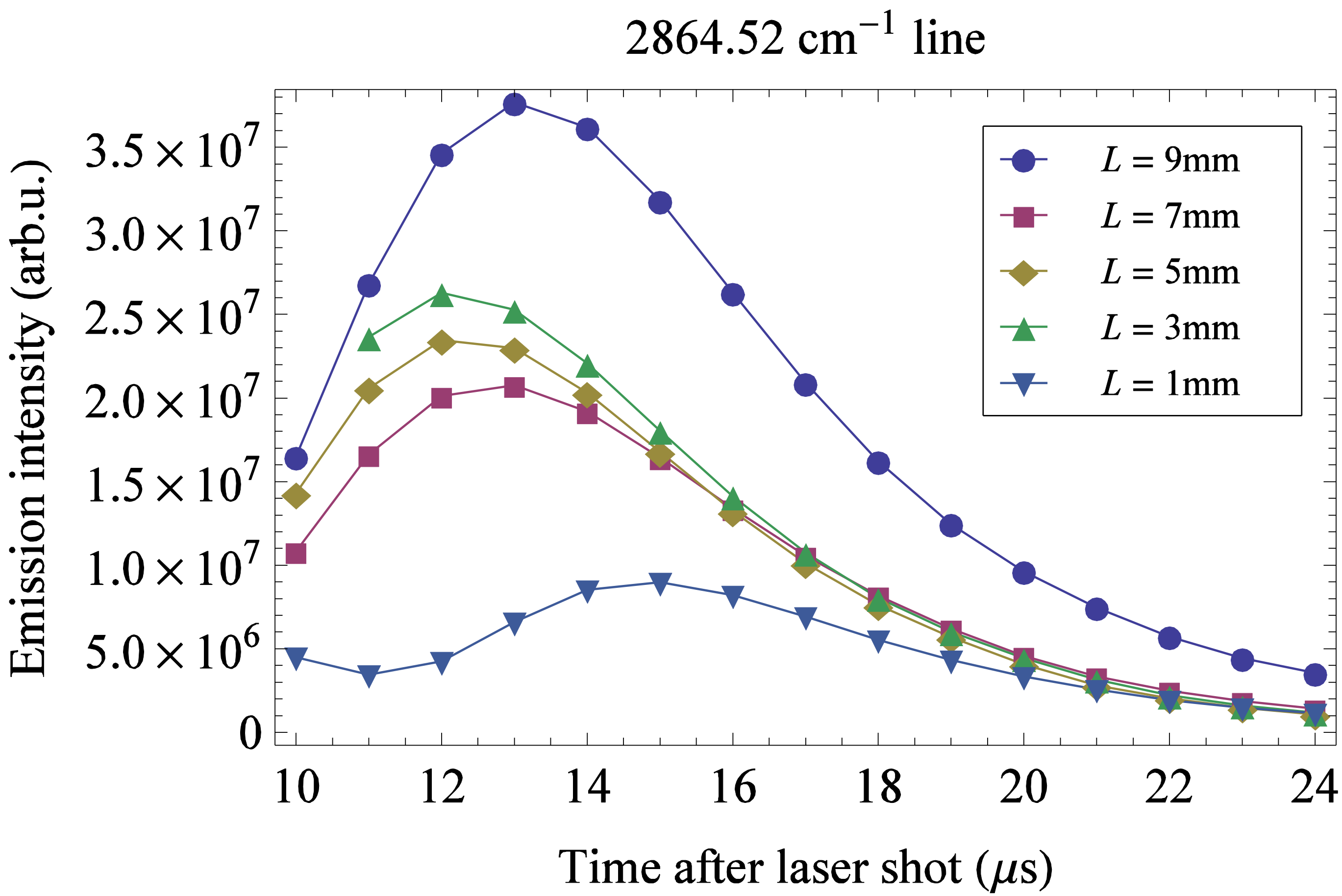

Spektrometr s Fourierovou transformací

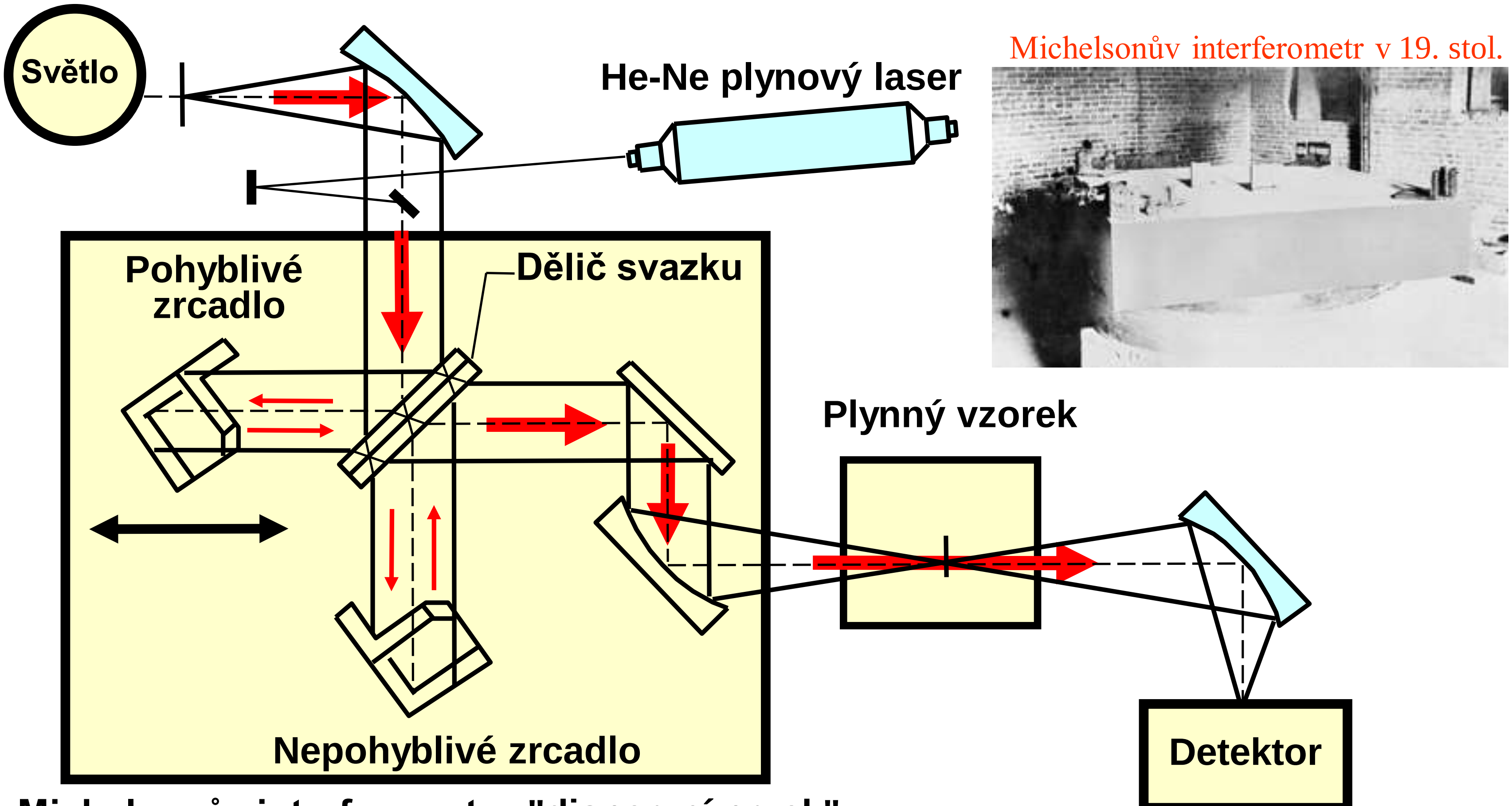

Michelsonův interferometr - "disperzní prvek"

Michelsonův interferometr v 19. stol.

Interference při pohybu zrcadla